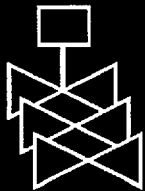
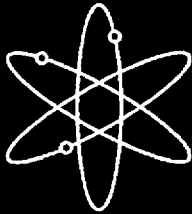
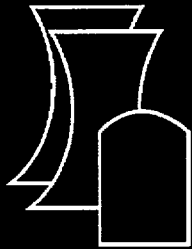


Evaluation of the Hualien Quarter Scale Model Seismic Experiment

Response of the Model to Seismic Events

City College of New York

**U.S. Nuclear Regulatory Commission
Office of Nuclear Regulatory Research
Washington, DC 20555-0001**



AVAILABILITY OF REFERENCE MATERIALS IN NRC PUBLICATIONS

NRC Reference Material

As of November 1999, you may electronically access NUREG-series publications and other NRC records at NRC's Public Electronic Reading Room at www.nrc.gov/NRC/ADAMS/index.html.

Publicly released records include, to name a few, NUREG-series publications; *Federal Register* notices; applicant, licensee, and vendor documents and correspondence; NRC correspondence and internal memoranda; bulletins and information notices; inspection and investigative reports; licensee event reports; and Commission papers and their attachments.

NRC publications in the NUREG series, NRC regulations, and *Title 10, Energy*, in the Code of *Federal Regulations* may also be purchased from one of these two sources.

1. The Superintendent of Documents
U.S. Government Printing Office
Mail Stop SSOP
Washington, DC 20402-0001
Internet: bookstore.gpo.gov
Telephone: 202-512-1800
Fax: 202-512-2250
2. The National Technical Information Service
Springfield, VA 22161-0002
www.ntis.gov
1-800-553-6847 or, locally, 703-605-6000

A single copy of each NRC draft report for comment is available free, to the extent of supply, upon written request as follows:

Address: Office of the Chief Information Officer,
Reproduction and Distribution
Services Section

U.S. Nuclear Regulatory Commission
Washington, DC 20555-0001

E-mail: DISTRIBUTION@nrc.gov

Facsimile: 301-415-2289

Some publications in the NUREG series that are posted at NRC's Web site address www.nrc.gov/NRC/NUREGS/indexnum.html are updated periodically and may differ from the last printed version. Although references to material found on a Web site bear the date the material was accessed, the material available on the date cited may subsequently be removed from the site.

Non-NRC Reference Material

Documents available from public and special technical libraries include all open literature items, such as books, journal articles, and transactions, *Federal Register* notices, Federal and State legislation, and congressional reports. Such documents as theses, dissertations, foreign reports and translations, and non-NRC conference proceedings may be purchased from their sponsoring organization.

Copies of industry codes and standards used in a substantive manner in the NRC regulatory process are maintained at—

The NRC Technical Library
Two White Flint North
11545 Rockville Pike
Rockville, MD 20852-2738

These standards are available in the library for reference use by the public. Codes and standards are usually copyrighted and may be purchased from the originating organization or, if they are American National Standards, from—

American National Standards Institute
11 West 42nd Street
New York, NY 10036-8002
www.ansi.org
212-642-4900

Legally binding regulatory requirements are stated only in laws; NRC regulations; licenses, including technical specifications; or orders, not in NUREG-series publications. The views expressed in contractor-prepared publications in this series are not necessarily those of the NRC.

The NUREG series comprises (1) technical and administrative reports and books prepared by the staff (NUREG-XXXX) or agency contractors (NUREG/CR-XXXX), (2) proceedings of conferences (NUREG/CP-XXXX), (3) reports resulting from international agreements (NUREG/IA-XXXX), (4) brochures (NUREG/BR-XXXX), and (5) compilations of legal decisions and orders of the Commission and Atomic and Safety Licensing Boards and of Directors' decisions under Section 2.206 of NRC's regulations (NUREG-0750).

DISCLAIMER: This report was prepared as an account of work sponsored by an agency of the U.S. Government. Neither the U.S. Government nor any agency thereof, nor any employee, makes any warranty, expressed or implied, or assumes any legal liability or responsibility for any third party's use, or the results of such use, of any information, apparatus, product, or process disclosed in this publication, or represents that its use by such third party would not infringe privately owned rights.

Evaluation of the Hualien Quarter Scale Model Seismic Experiment

Response of the Model to Seismic Events

Manuscript Completed: October 2000
Date Published: March 2001

Prepared by
C. A. Miller, C. J. Costantino

City College of New York
Earthquake Research Center
Department of Civil Engineering
New York, NY 10031

H. L. Graves, NRC Project Manager

Prepared for
Division of Engineering Technology
Office of Nuclear Regulatory Research
U.S. Nuclear Regulatory Commission
Washington, DC 20555-0001
NRC Job Code W6769



ABSTRACT

This report is the fourth volume of a four volume set describing the work performed in evaluating the results obtained from the Hualien quarter scale model seismic experiments. The results discussed in this volume relate to the response of the structure to the seismic events recorded at the site.

Data has been collected for a series of earthquakes which have occurred at the Hualien site over the past several years. Most of these events have resulted in peak ground accelerations recorded at the site which are somewhat less than 0.1 g. Accelerograms have been collected throughout the model structure and in the free field. Downhole instrumentation is in place for depths up to 170'. This report discusses results for two earthquakes.

The measured data were studied to evaluate the structural system characteristics. The measured downhole free field accelerations were compared with predicted accelerations using vertically propagating shear wave theory as contained in the CARES code. The agreement was fairly good. The CARES computer code was also used to predict the motion of the model. These predictions did not agree very well with the measured results. The major cause of the disagreement is attributed to the anisotropic characteristics of the site.

The volumes contained in this report, "Evaluation of the Hualien Quarter Scale Model Seismic Experiment," are:

- | | |
|--------|--|
| Vol. 1 | Description of Experiment and Summary of Results |
| Vol. 2 | Geotechnical Site Characterization Review |
| Vol. 3 | Results of the Forced Vibration Tests |
| Vol. 4 | Response of the Model to Seismic Events |

TABLE OF CONTENTS

Abstract	iii
Table of Contents	v
List of Figures	vi
List of Tables	ix
Acknowledgement	x
1.0 Introduction	1
2.0 Description of Experiment and Earthquakes	3
2.1 Experiment Description	3
2.2 Earthquake Descriptions	4
2.3 Transfer Functions Between Structure and Free Field	5
3.0 Measured Data	21
3.1 Transfer Functions Between Stations in the Downhole Array	21
3.2 Transfer Functions Between the Model and Free Field	23
4.0 Correlation of Predicted with Measured Free Field Response	37
5.0 Correlation of Predicted with Measured Model Response	49
6.0 Summary and Conclusions	59
References	63

LIST OF FIGURES

Fig. 2.1	Sketch of Hualien Model	8
Fig. 2.2	Site Plan and Principal Response Directions	9
Fig. 2.3	Spectra (5%) of Motion Recorded at Gages a25 During 1-20-94 Earthquake	10
Fig. 2.4	Spectra (5%) of Motion Recorded at Gages a25 During 2-23-95 Earthquake	11
Fig. 2.5	Spectra (5%) of Motion Recorded at Gages a25 During 5-1-95 Earthquake	12
Fig. 2.6	Spectra (5%) of Motion Recorded at Gages a25 During 5-2-95 Earthquake	13
Fig. 2.7	Identification of Measured Responses in the Free Field and Model	14
Fig. 2.8	Mohr Circle Transformation from L, T Coordinates to X, Y Coordinates	14
Fig. 2.9	Roof Longitudinal Response / Free Field Input - February 23, 1995	15
Fig. 2.10	Roof Coupled Response / Free Field Input - February 23, 1995	15
Fig. 2.11	Roof Transverse Response / Free Field Input - February 23, 1995	16
Fig. 2.12	Principal Angle Derived From Roof Data - February 23, 1995	16
Fig. 2.13	Roof "X" Response / Free Field Input - February 23, 1995	17
Fig. 2.14	Roof "Y" / Free Field Input - February 23, 1995	17
Fig. 2.15	Roof Longitudinal Response / Free Field Input - May 1, 1995	18
Fig. 2.16	Roof Coupled Response / Free Field Input - May 1, 1995	18
Fig. 2.17	Roof transverse Response / Free Field Input - May 1, 1995	19
Fig. 2.18	Principal Angle Derived From Roof Data - May 1, 1995	19

Fig. 2.19 Roof "X" Response / Free Field Input - May 1, 1995	20
Fig. 2.20 Roof "Y" / Free Field Input - May 1, 1995	20
Fig. 3.1 Transfer Functions a25/d25; 2-23-95	25
Fig. 3.2 Transfer Functions d25/d26; 2-23-95	26
Fig. 3.3 Transfer Functions d26/d27; 2-23-95	27
Fig. 3.4 Transfer Functions d27/d28; 2-23-95	28
Fig. 3.5 Transfer Functions a25/d25; 5-1-95	29
Fig. 3.6 Transfer Functions d25/d26; 5-1-95	30
Fig. 3.7 Transfer Functions d26/d27; 5-1-95	31
Fig. 3.8 Transfer Functions d27/d28; 5-1-95	32
Fig. 3.9 L Transfer Functions Between Roof and Furthest Free Field Gages; 2-23-95	33
Fig. 3.10 T Transfer Functions Between Roof and Furthest Free Field Gages; 2-23-95	34
Fig. 3.11 X Transfer Functions Between Roof and Furthest Free Field Gages; 2-23-95	35
Fig. 3.12 Y Transfer Functions Between Roof and Furthest Free Field Gages; 2-23-95	36
Fig. 4.1 Soil Column Model Used for Convolution Analyses	41
Fig. 4.2 Comparison of Computed and Measured Free Field X Spectra (5%); 2-23-95	42
Fig. 4.3 Comparison of Computed and Measured Free Field Y Spectra (5%); 2-23-95	43
Fig. 4.4 Comparison of Computed and Measured Free Field V Spectra (5%); 2-23-95	44
Fig. 4.5 Comparison of Computed and Measured Free Field X Spectra (5%); 5-1-95	45

Fig. 4.6	Comparison of Computed and Measured Free Field Y Spectra (5%); 5-1-95	46
Fig. 4.7	Comparison of Computed and Measured Free Field V Spectra (5%); 5-1-95	47
Fig.5.1	Comparison of Computed with Measured Model X Spectra (5%); 2-23-95	52
Fig.5.2	Comparison of Computed with Measured Model Y Spectra (5%); 2-23-95	53
Fig.5.3	Comparison of Computed with Measured Model V Spectra (5%); 2-23-95	54
Fig.5.4	Comparison of Computed with Measured Model X Spectra (5%); 5-1-95	55
Fig.5.5	Comparison of Computed with Measured Model Y Spectra (5%); 5-1-95	56
Fig.5.6	Comparison of Computed with Measured Model V Spectra (5%); 5-1-95	57

LIST OF TABLES

Table 2.1	Characteristics of the Earthquakes	4
Table 3.1	Characteristics of Soil Column Transfer Functions (2-23-95)	21
Table 3.2	Estimates of Shear Velocity (fps) and Damping (%) (2-23-95)	22
Table 3.3	Characteristics of Soil Column Transfer Functions (5-1-95)	23
Table 4.1	Peak Shear Strains for February 1995 Earthquake	38
Table 4.2	Peak Shear Strains for May 1, 1995 Earthquake	40
Table 5.1	Soil Shear Moduli (ksf) Used for February 23, 1995 Event	49
Table 5.2	Soil Shear Moduli (ksf) Used for May 1, 1995 Event	51

ACKNOWLEDGEMENT

The authors wish to acknowledge the contributions to this project made by Applied Research Associates (ARA) who are subcontractors to CCNY on the study. Drs. C.N. Higgins and J. Pires of ARA made significant contributions to this report. Research Associates at CCNY who participated in the work reported here are: E. Heymsfield, S. Jaysena, J. McClean, A. Mousa, A. Yang, and Y. Zhu.

A special acknowledgement is given to the NRC Project Manager, Mr. Herman Graves. He actively participated in all aspects of the program. Recognition is also due to Dr. H.Tang of the Electric Power Research Institute who is directing the consortium of researchers conducting the Hualien project.

1.0 Introduction

This report is submitted on Contract No. NRC-04-92-049, "Hualien SSI Experiment." It covers a portion of the work performed on a review of the results obtained from earthquakes recorded at the site. The work was performed from March 1994 through February 1997. This is the fourth of four volumes comprising the final report on the program. A listing of the title for each of the volumes is given in the Abstract.

A soil structure interaction (SSI) experiment is being conducted in Hualien, Taiwan. A quarter scale model reactor containment building model has been constructed at a seismically active site in Hualien. The structure and free field are instrumented so that response data within the structure and in the free field can be obtained for seismic events occurring at the site. Forced vibration tests have been performed to evaluate vibration characteristics of the combined soil-structure system. Two such tests were performed, one before the backfill was placed and the second after the backfill was placed. These tests are discussed in the third volume to this report. This experiment is similar to the recently completed experiment at Lotung (Ref. 1). The soil at the Lotung site was rather soft (having a shear wave velocity of about 350 fps) while the Hualien soil is relatively stiff (having a shear wave velocity of about 1000 fps). The objective of the City College of New York (CCNY) contract is to provide support to NRC in planning the experiment and in evaluating the results. Applied Research Associates (ARA) is a subcontractor to CCNY on the project.

The objective of the work reported in this volume is to review the results obtained from four earthquakes. This review includes two tasks. The first task is to correlate the measured free field data with predictions made using convolution methods. The CARES code (Ref. 2) is used to make the predictions. This is discussed in Section 4 of the report. The second task is to correlate the measured structural response data with predicted responses using standard soil-structure-interaction methodologies. The CARES code is again used to make the predictions. These correlations are discussed in Section 5. The results of these reviews are summarized in Section 6. A brief description of the four earthquakes considered in this report is given in Section 2. The measured data are discussed in Section 3. The instrumentation in both the free field and in the structure is also described in Section 2.

A surface water filled tank has also been constructed at the site. Data was available for an October 1995 event, but the water level in the tank was not measured at the time of the event. No work was therefore done on the tank.

2.0 Description of Experiment and Earthquakes

The site characteristics and earthquakes considered in the review are discussed in this section of the report. A general description of the structure and site is given in Volume 1; only brief summaries of the site, instrumentation, and structural description are included here for convenience. The forced vibration tests indicated (see volume 3 of this report) that the site soil properties are likely anisotropic (i.e., are orientation sensitive in a horizontal plane). Transfer functions between the structural and the free field motion are used to investigate the extent to which these effects are evident in the earthquake response measurements. This work is also described in this section of the report.

2.1 Experiment Description

The quarter scale model containment structure is located at Hualien in an area of high seismicity along the east coast of Taiwan. A sketch of the model and the significant soil properties are shown on Figure 2.1. The soil properties are as recommended by CRIEPI for the "unified model" and are discussed in Volume 2. It should be noted that the use of these properties resulted in good correlation between the measured and computed responses for the forced vibration tests as discussed in Volume 3.

The structural model instrumentation consists of accelerometers located at the north end, east end, south end, west end and center of the roof and at the north end, east end, south end, and west end of the basemat. These accelerometers are tridirectional recording horizontal motion in the L, and T directions and vertical (V) direction. The L direction corresponds to north.

The free field instrumentation that has been in place to record the seismic motions is shown on Figure 2.2a. As may be seen this instrumentation is located along three radial arms: arm 1 is oriented 60.7° west of north (L); arm 2 is oriented south east from the model; and arm 3 is oriented north east from the model. The North direction for the shaker tests was designated to be oriented $N 30.7^\circ W$ from the model as shown.

Each of the radial arms contains five surface stations located at 0.5, 1, 2, 3, and 5.5 diameters from the center of the model. The outer three locations are located outside the backfill region. Three accelerometers are placed at each location collecting accelerograms in the three directions (L, T, and V). The surface gages are designated (aijk) where i is the arm (1, 2, or 3), j is the radial location (1...5), and k indicates the direction of the recording (L, T, or V). When required for clarity this gage number is preceded in this report with the date of the earthquake for which the recording was made.

Downhole measurements are taken at three locations (below gages a21, a25, and a15) as shown on Figure 2.2 b. There are four gages in each hole located at depths of: 17.33', 51.84', 86.29', and 170.6'. Motion in the L, T, and V directions are also recorded at each of these gages. These gages are designated as dmn with mn of the top gage equal to the ij of the surface gage above it and the mn increasing by one for each gage moving down the hole.

2.2 Earthquake Descriptions

Many earthquakes but been recorded at the site but four have been selected for detailed study. These four were selected based on completeness of the collected data, and the characteristics of the earthquake (frequency content, and magnitude of the motions induced at the site). Descriptions of the earthquakes are shown on Table 2.1. As may be seen the first two earthquakes are quite similar in magnitude, distance from the site, and depth. They also both induce similar peak accelerations at the site on in the model. The last two earthquakes are also similar to each other having similar magnitudes, occurring close to the site, and located at shallow depths. It is surprising that the May 2 event resulted in significantly lower response at both the site and in the model.

Table 2.1

Characteristics Of The Earthquakes

Date	Moment Magnitude	Location From Model		Epicentral Depth (km)	Peak Accelerations (G)	
		Distance (km)	Azimuth		Free Field	Structural
1-20-94	5.6	24.4	77.5°	49.5	0.05	0.08
2-23-95	5.8	21.8	18.8°	21.7	0.05	0.06
5- 1-95	4.9	4.6	48.7°	8.4	0.14	0.17
5- 2-95	4.6	1.7	107.7°	8.9	0.09	0.08

Spectra of the motion at station a25 are shown on Figures 2.3 through 2.6 for the four earthquakes. As may be seen from Figure 2.3 the January 10 earthquake resulted in about equal motion in the L and T directions with the frequency content in the L direction being somewhat

higher than in the T direction. The spectra (Figure 2.4) of the February 23 event are less broad than the prior event. These spectra show peaks at about 1.5 cps and 7.5 cps in the longitudinal direction and about 1.3 cps and 3 cps in the transverse direction. The peak amplification in the vertical direction is at a frequency of about 25 cps. The spectra of the two May events are shown on Figures 2.5 and 2.6. The May 1 event horizontal spectra are rather broad banded while the horizontal spectra for the May 2 event are narrow banded with both the (L) and (T) spectra showing peaks occurring at about 9 cps. The both events have large vertical components which occur at about 25 cps.

Based upon the earthquake characteristics discussed above the February 23, 1995 and May 1, 1995 are selected for detailed study.

2.3 Transfer Functions Between Structure and Free Field

The results of the shaker tests indicated that the site may be anisotropic in that shaker motion in one direction caused significant motion in a direction normal to the input energy. This occurred even though the model is axisymmetric. The extent to which these anisotropic characteristics of the site are reflected in the earthquake data is investigated by comparing the transfer functions between the model response and the free field. If the site were isotropic, transfer functions relating the model response (in either the L or T directions) to the free field motion would be expected to be the same. The transfer functions would also be expected to be independent of the free field surface gage used as a control point. In the following analysis the model response is related to the free field response by three transfer functions: L model response divided by L free field input (H_{LL}); T model response divided by T free field input (H_{TT}); and L model response divided by T free field input (H_{LT}). These transfer functions are derived by from the measured model response and the nine surface free field gages located outside of the backfill. A least squared error criterion is used to determine "average" transfer functions between the model response and each of the nine free field gages. The site is considered to be anisotropic when H_{LT} is non zero and when H_{LL} is not equal to H_{TT} . Principal directions of the site are then evaluated so that H_{LT} equals zero.

Figure 2.7 identifies the notation used for the measured data in the structure and in the free field. The parameter (k) indicates the free field gage number (e.g., a25). The x,y coordinate system represents the principal directions as will be discussed below.

At each frequency (ω) the structural response can be written as:

$$\begin{aligned}
 R_L &= H_{LL} F_{Lk} + H_{LT} F_{Tk} \\
 R_T &= H_{LT} F_{Lk} + H_{TT} F_{Tk}
 \end{aligned}
 \tag{2.1}$$

Of course, $H_{LL} = H_{TT}$ and $H_{LT} = 0$ for an isotropic material.

The transfer functions (H_{LL} , H_{LT} , H_{TT}) are then computed based on a least squared error fit to Eqs. (2.1) using all of the surface gages outside of the backfill (a13 through a15, a23 through a25, and a33 through a35) and the model responses. The real and imaginary parts of the transfer functions are evaluated but the amplitudes are used for the further analyses.

It is then assumed that principal directions exist such that the structural response can be written in the principal coordinate system as:

$$\begin{aligned}
 R_x &= H_{xx} F_{xk} \\
 R_y &= H_{yy} F_{yk}
 \end{aligned}
 \tag{2.2}$$

The transfer functions in the principal directions (H_{xx} and H_{yy}) are obtained from Mohr's circle (see Figure 2.8). This transformation also gives the angle (θ) between the principal (x,y) and the test directions (L,T)

These analyses are carried out for each of the frequencies and for the two earthquakes. The transfer function amplitudes obtained from the February 23, 1995 data between the roof of the model and the free field gages are shown on Figures 2.9 through 2.11 for the longitudinal, coupled, and transverse direction respectively. Each of these plots contains a fourth order best fit to give some sense of the average transfer values over some broad frequency range. It may be seen that the transfer function in the (L) direction tends to be larger than in the (T) direction, and the magnitude of the coupling transfer function is only slightly less than the transverse function.

The principal directions (X, Y) are then computed as discussed above with the results shown on Figure 2.12. It may be seen that the angle defining the principal directions varies from about 10° to 40° . The linear fit to the data, shown on the figure, indicates that an average angle is about 29° and is not a significant function of frequency. The transfer functions in the principal directions are then computed and plotted on Figures 2.13 and 2.14. The (Y) transfer functions are smaller

than the (X) functions indicating that the site is stiffer in the (Y) direction than it is in the (X) direction.

It is interesting to consider the orientation of the principal directions relative to the site geometry as shown on Figure 2.2a. The principal directions are shown relative to the (L, T) system with the 29° angle taken clockwise from the (L or north direction). Then as discussed above the (Y) principal direction is the stiffer of the two. It is interesting to recall that the maximum response (softer) principal direction for the FVT-2 test was found to be about 30° counterclockwise from the shaker north (also shown on Figure 2.2a). This is within one degree of the minimum principal direction as found here. Figure 2.2a may also give some indication of the reason for the nonisotropic conditions at the site. Mechanical vibrations radiate out from the plant shown on the figure. These vibrations could have consolidated the soil in the radial direction through the years. Radial lines from the plant are close to the stiffer principal direction at the site.

The May 1, 1995 earthquake is analyzed in the same manner using the roof response of the model as the reference response. The results are shown on Figures 2.15 through 2.20. The principal direction angle is once again found to be 29° (see Figure 2.18).

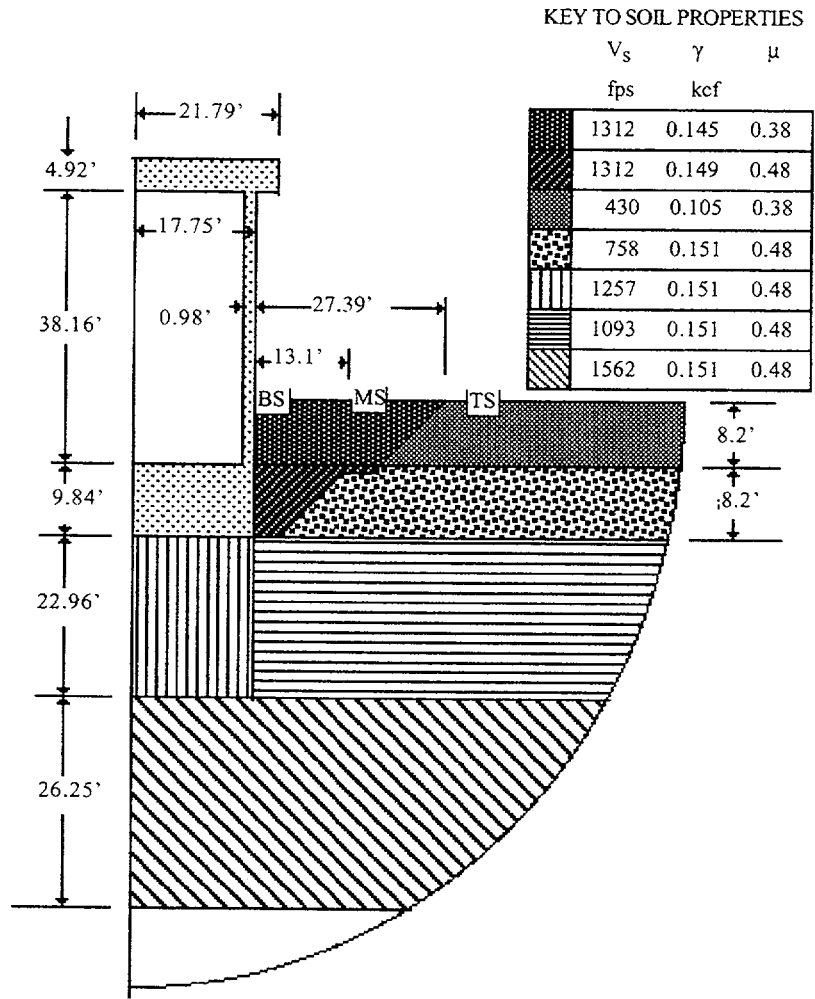


Fig. 2.1 Sketch of Hualien Model

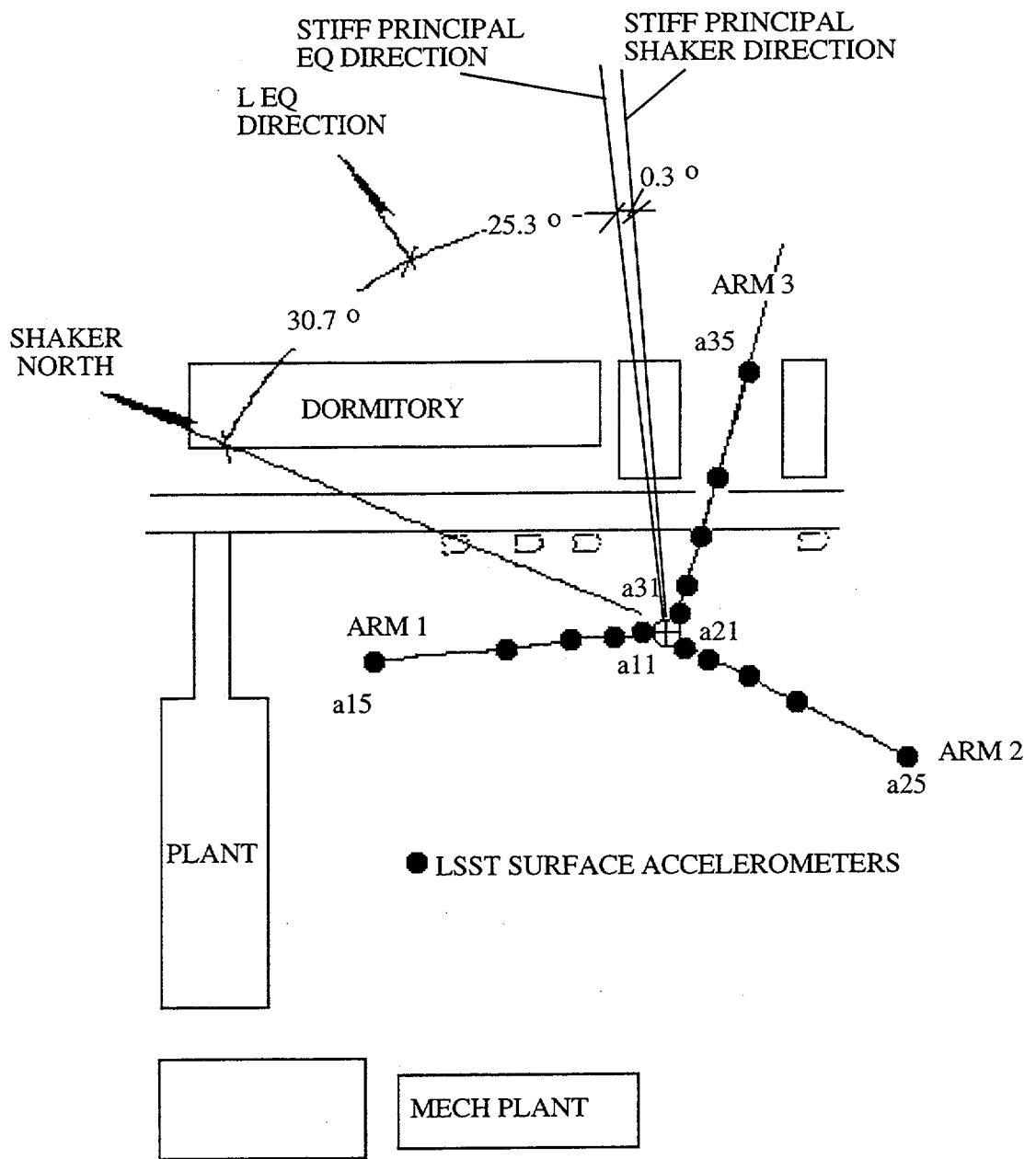


Fig. 2.2 Site Plan and Principal Response Directions

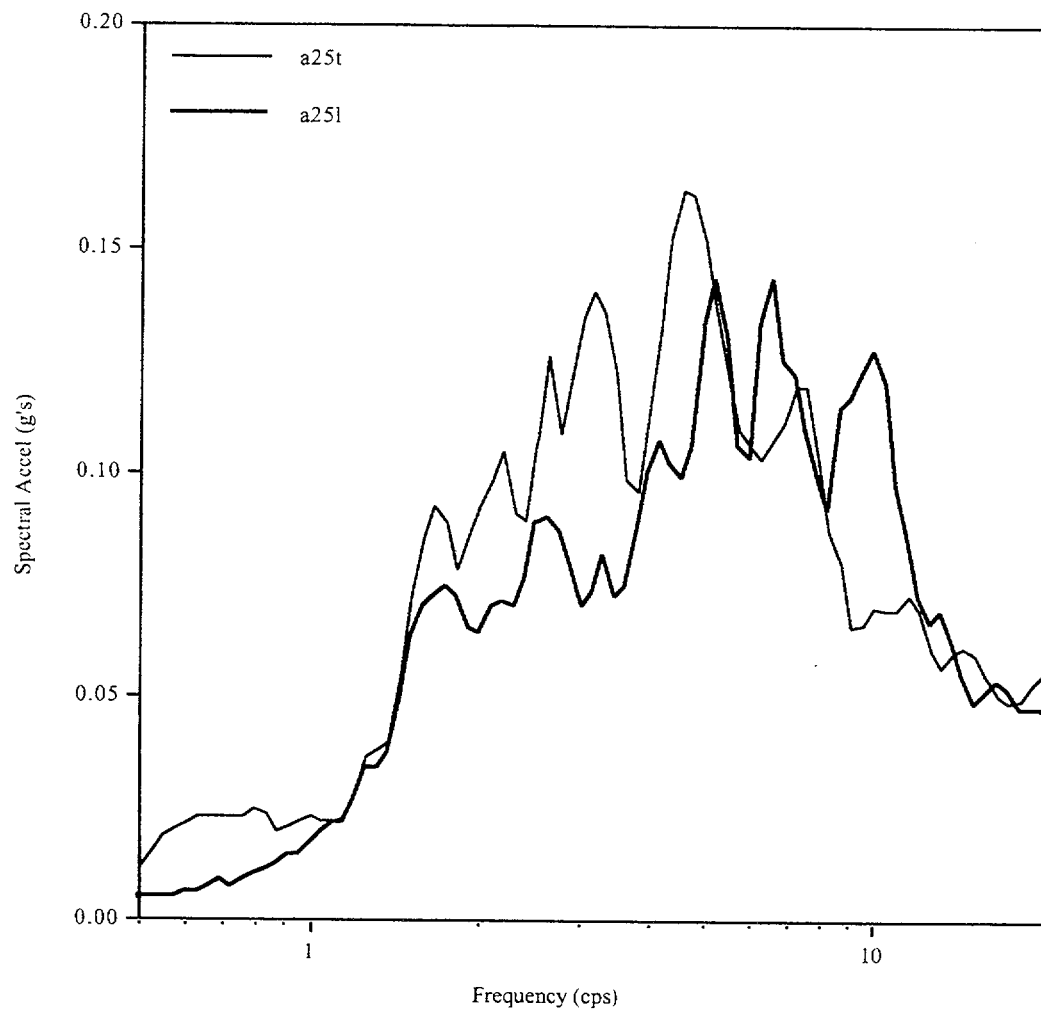


Fig. 2.3 Spectra (5 %) of Motion Recorded At Gages a25 During 1-20-94 Earthquake

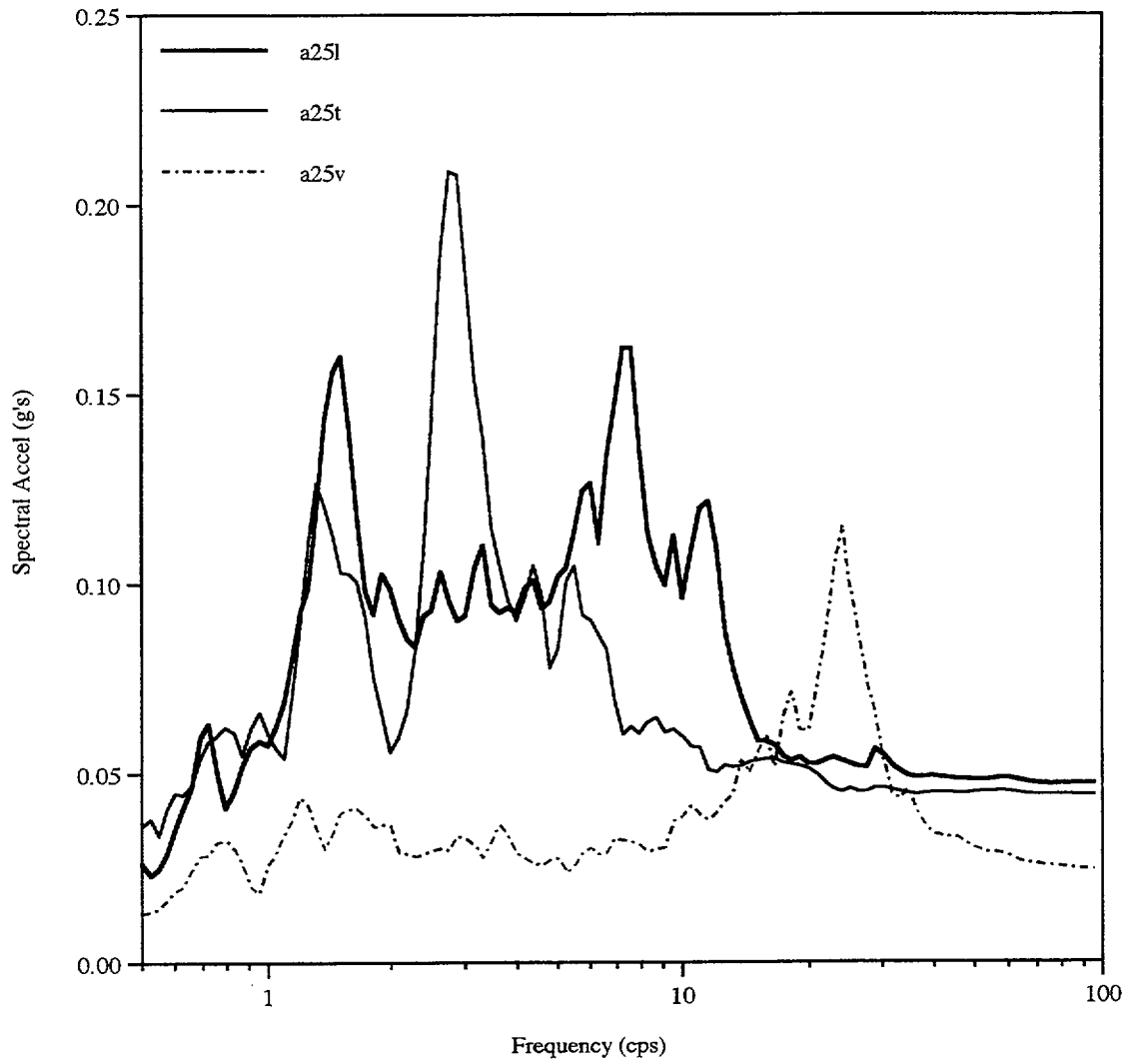


Fig. 2.4 Spectra (5 %) of Motions Recorded At Gages A25 During 2-23-95 Earthquake

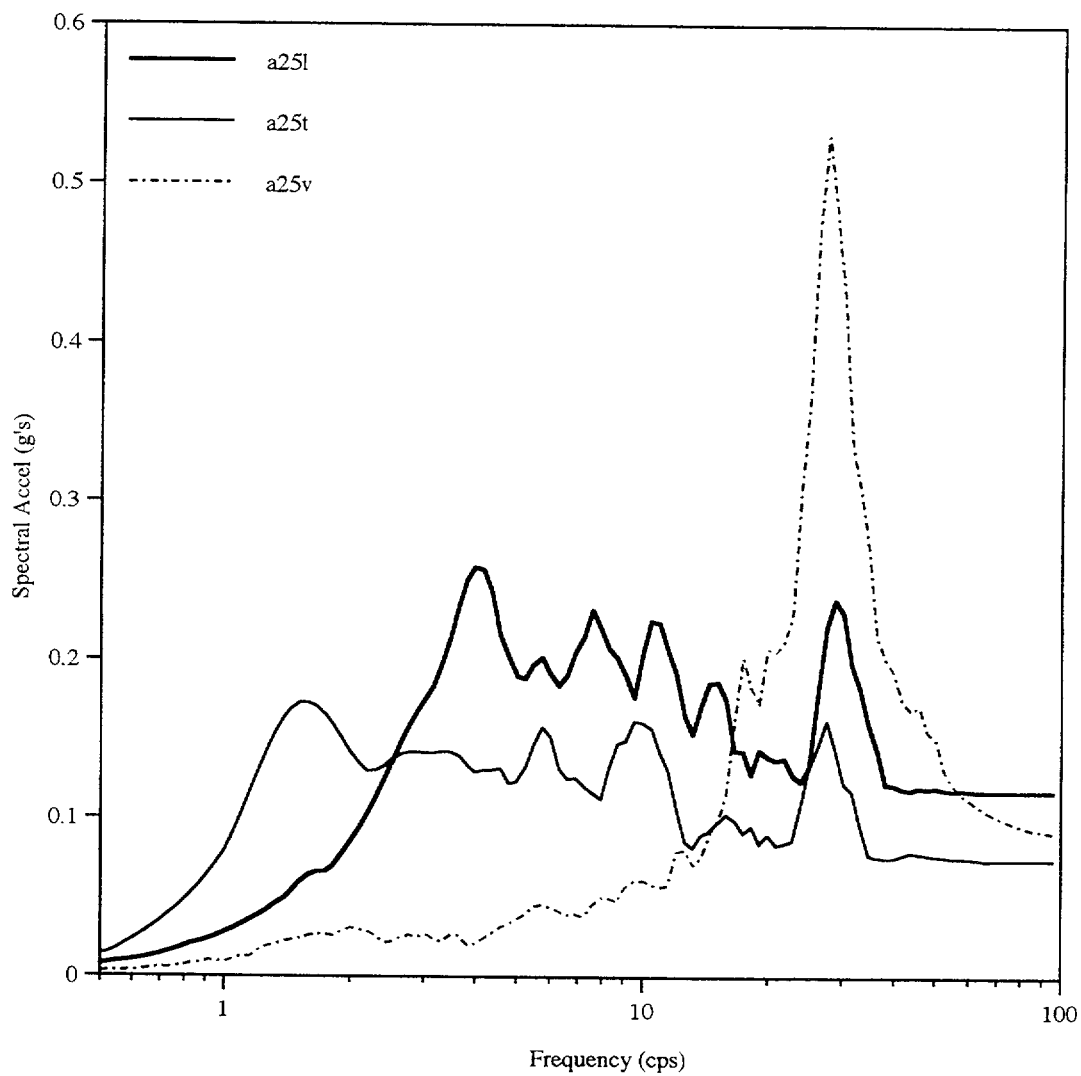


Fig. 2.5 Spectra (5%) of Motion Recorded at Gages a25 During 5-1-95 Earthquake

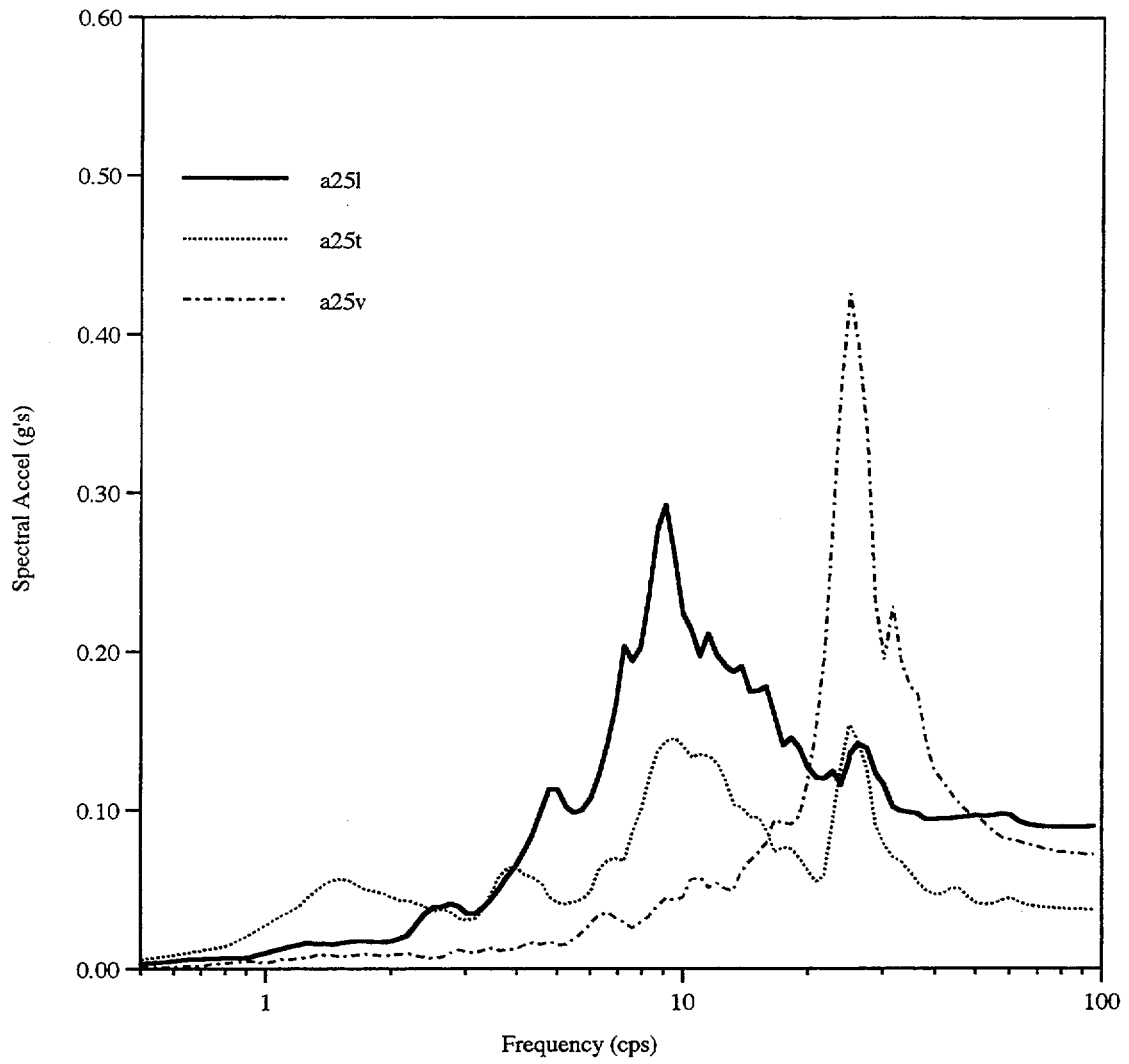


Fig. 2.6 Spectra (5%) of Motion Recorded at Gages a25 During 5-2-95 Earthquake

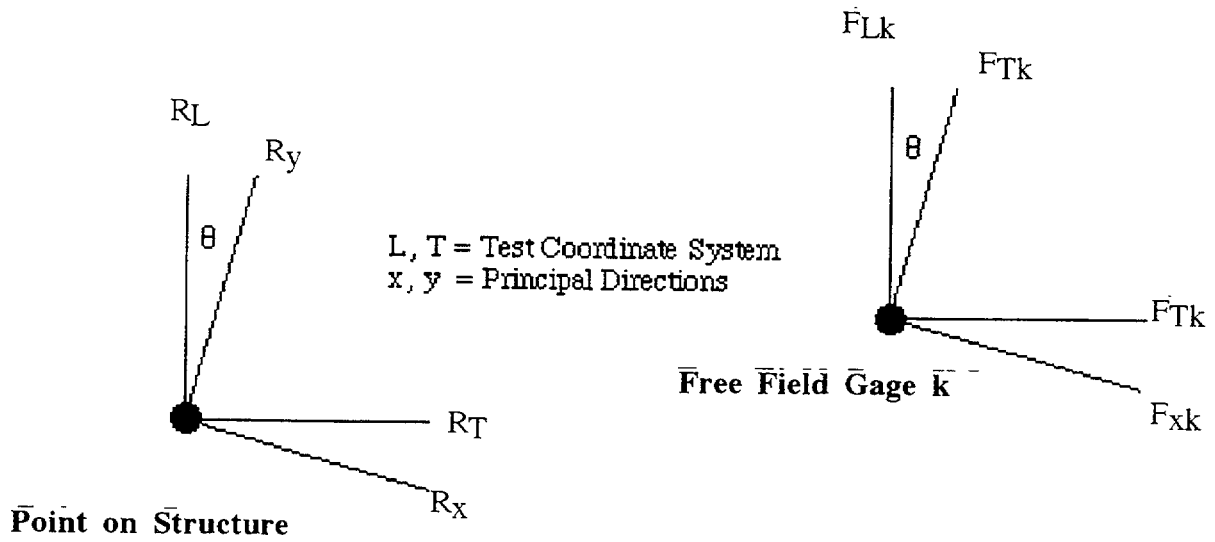


Fig. 2.7 Identification of Measured Responses in the Free Field and Model

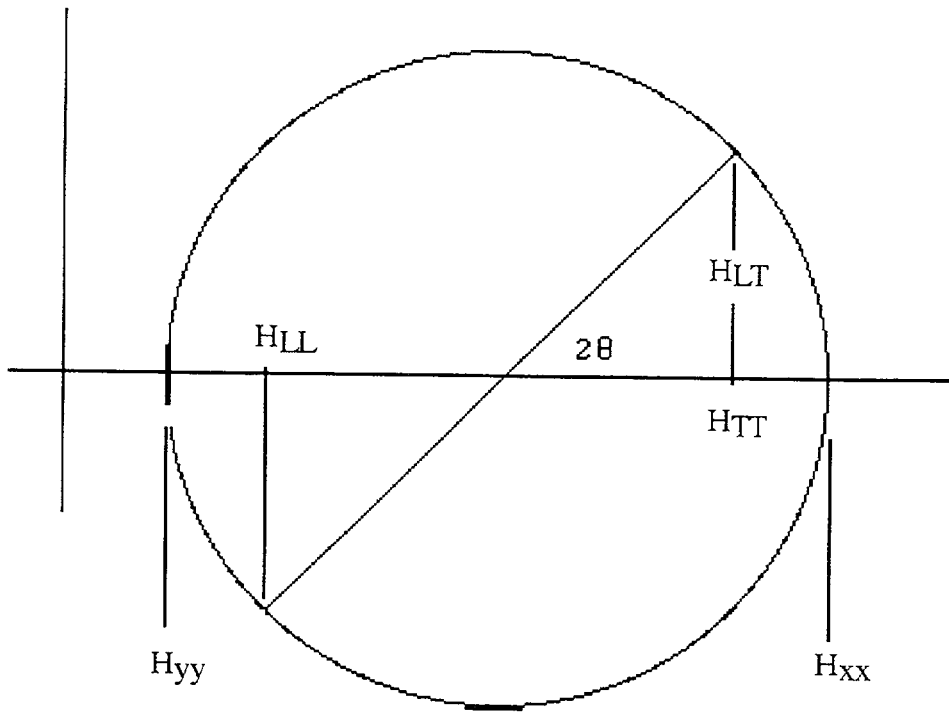


Fig. 2.8 Mohr Circle Transformation from L, T Coordinates to x, y Coordinates

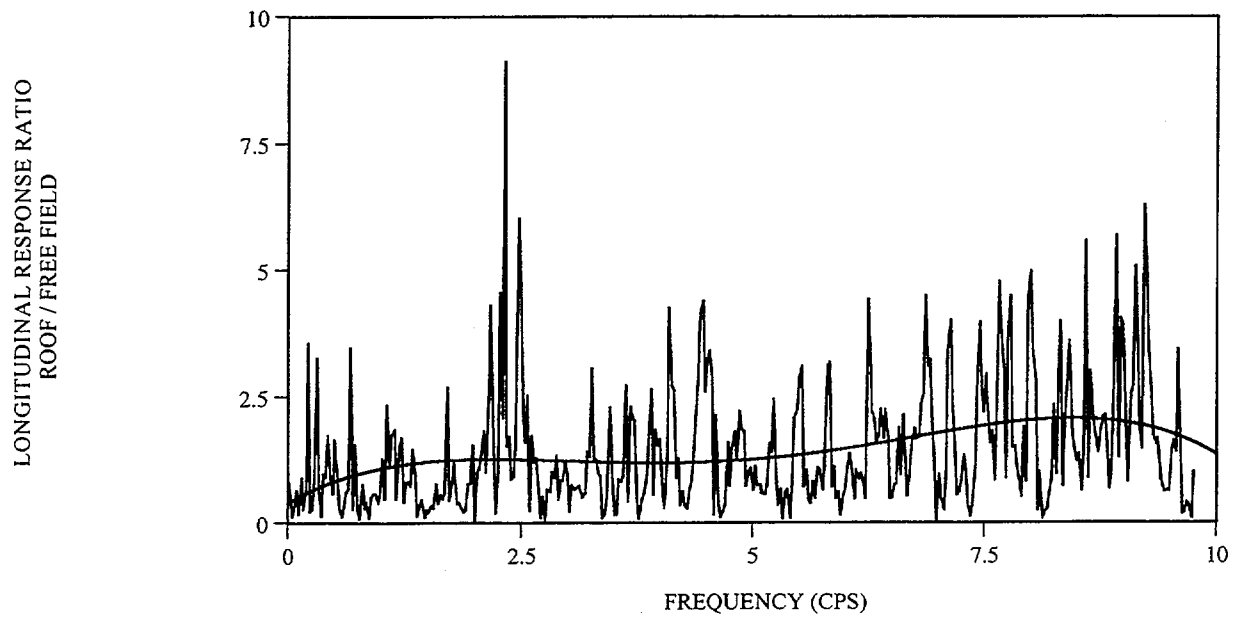


Figure 2.9 Roof Longitudinal Response / Free Field Input - February 23, 1995

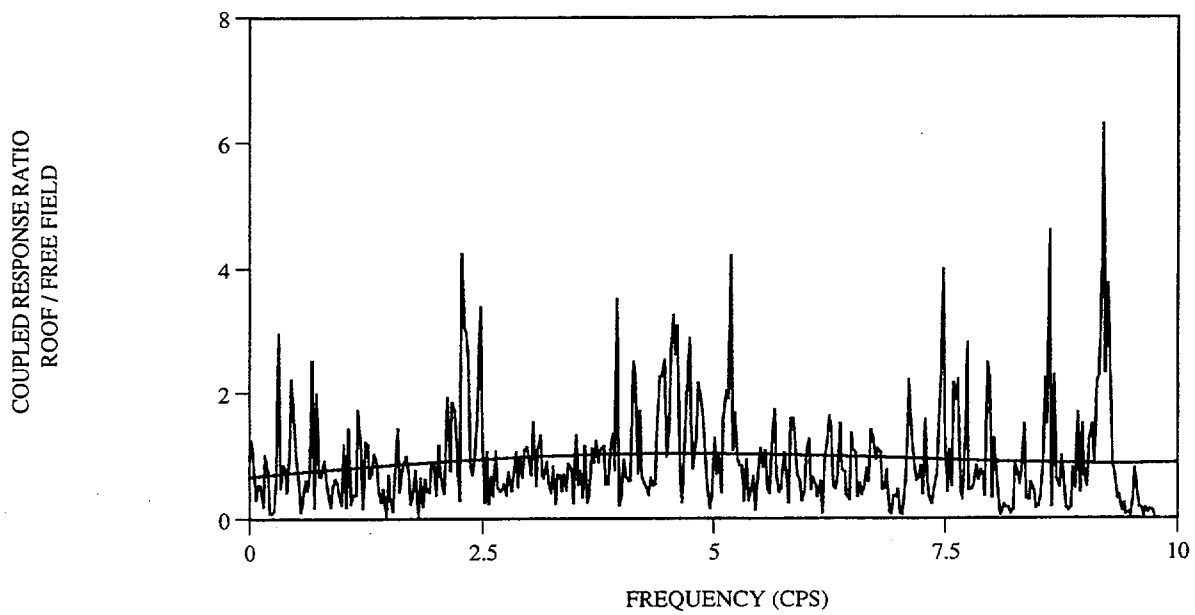


Figure 2.10 Roof Coupled Response / Free Field Input - February 23, 1995

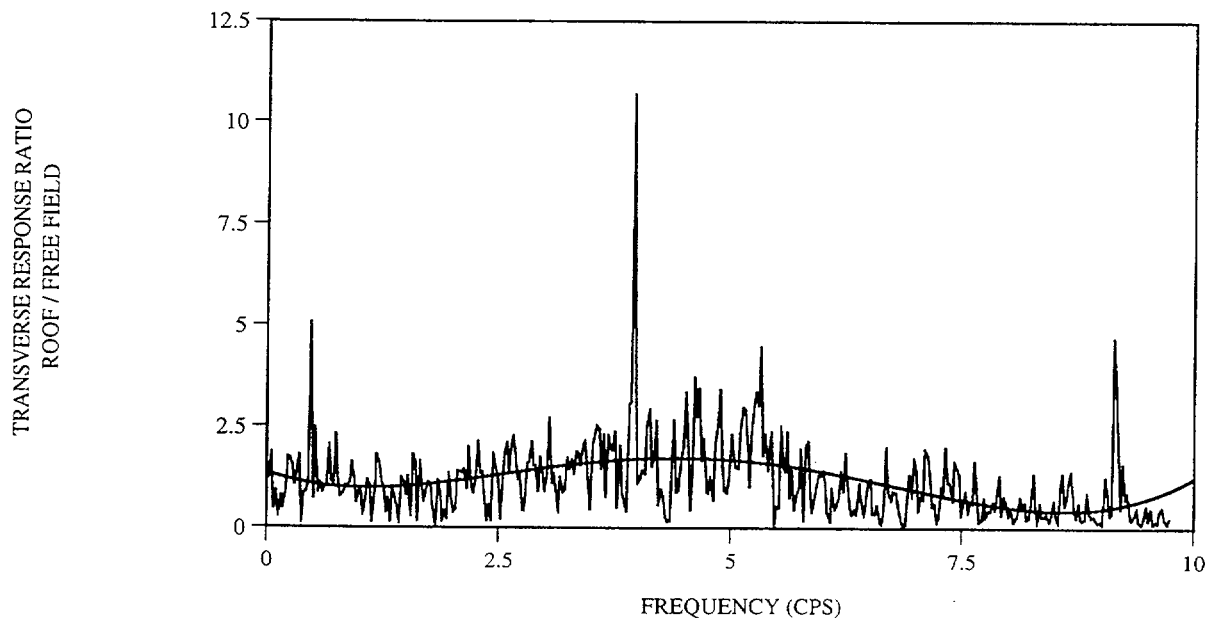


Figure 2.11 Roof Transverse Response / Free Field Input - February 23, 1995

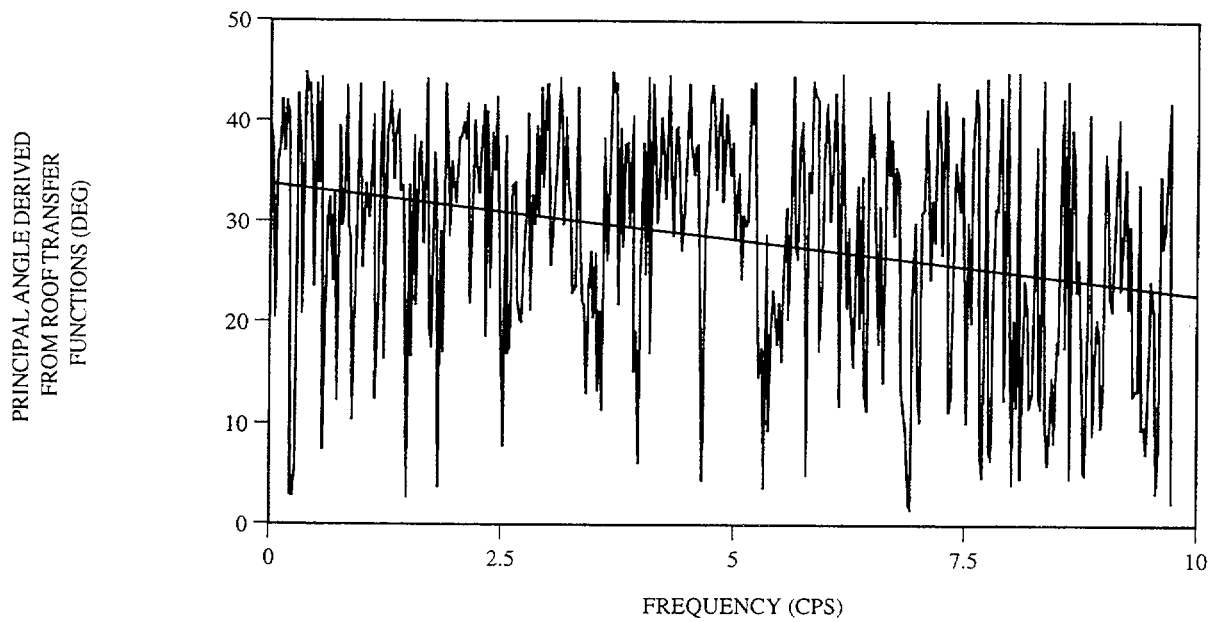


Figure 2.12 Principal Angle Derived From Roof Data - February 23, 1995

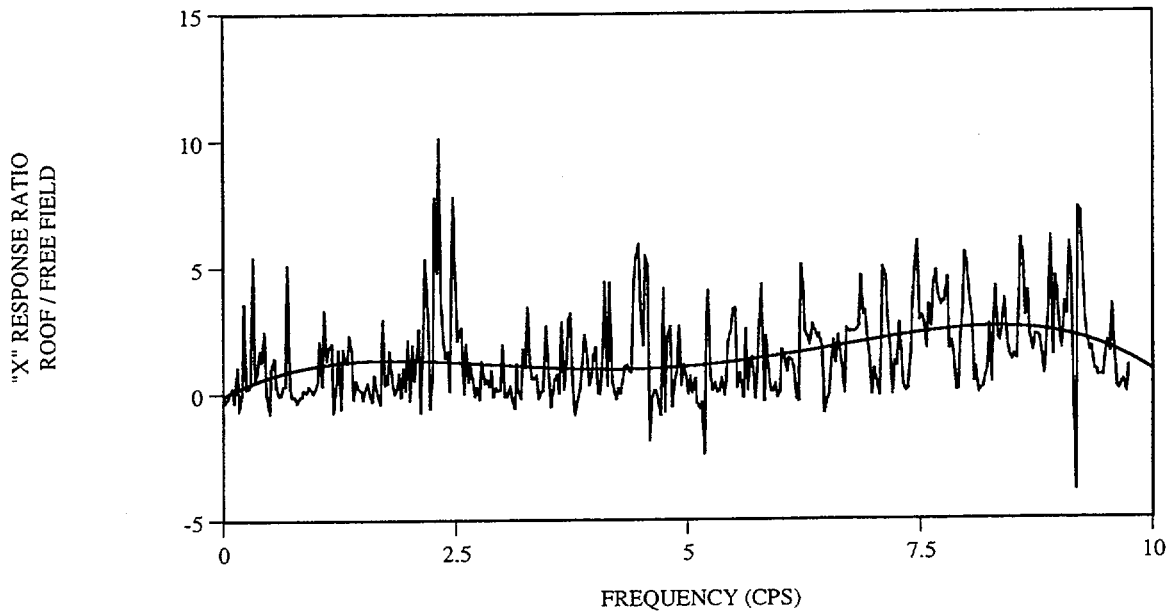


Figure 2.13 Roof "X" Response / Free Field Input - February 23, 1995

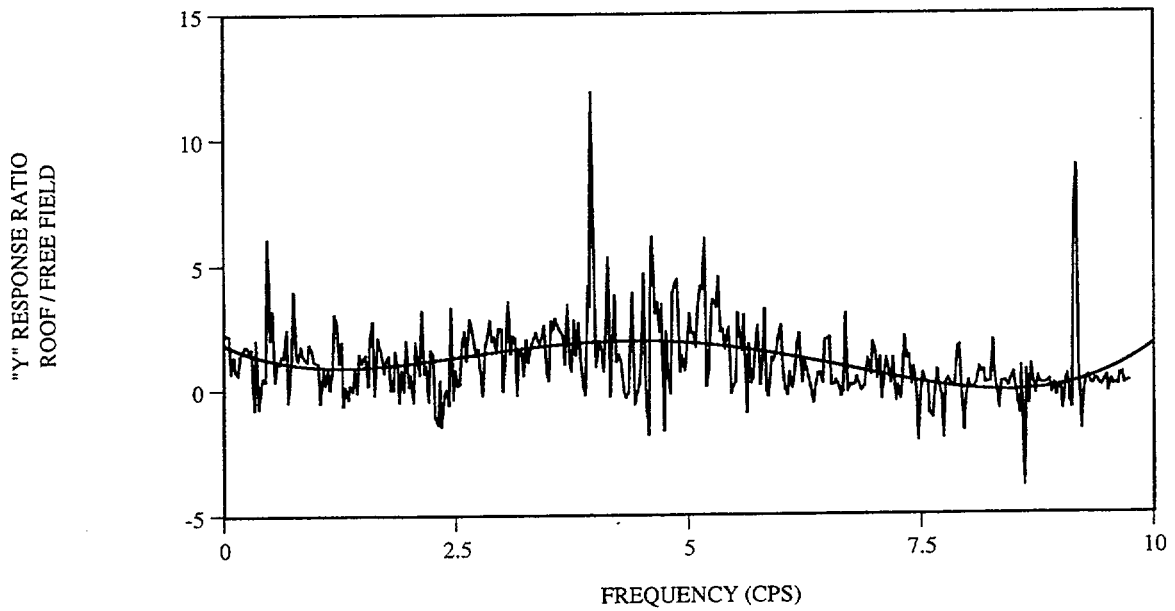


Figure 2.14 Roof "Y" Response / Free Field Input - February 23, 1995

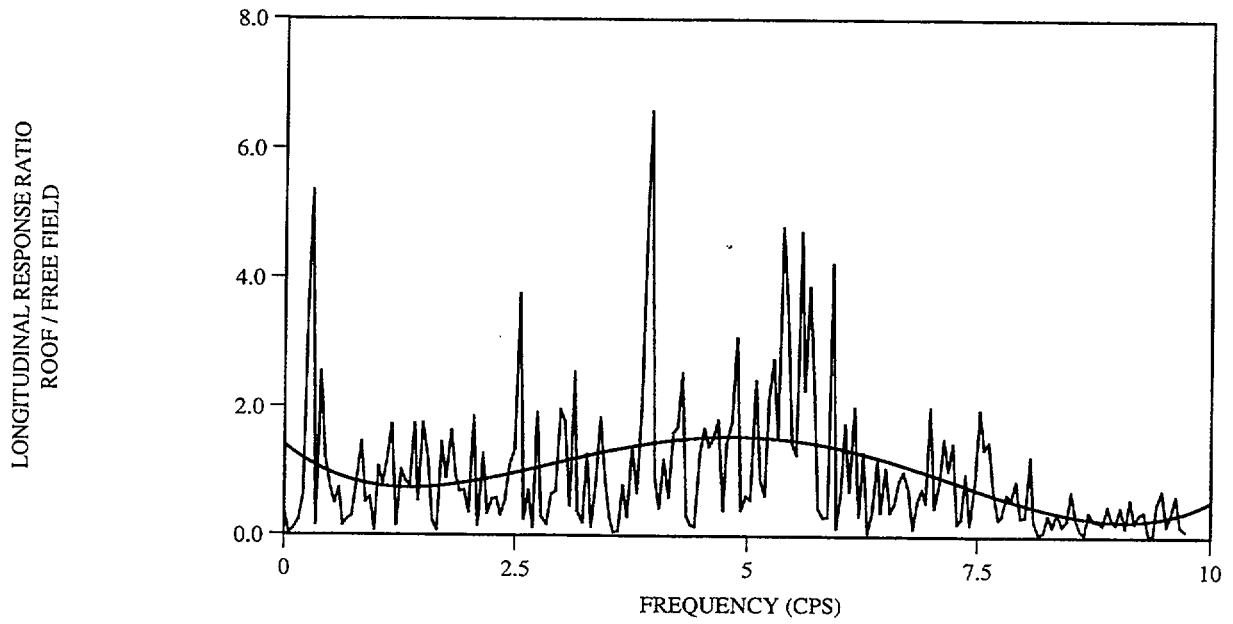


Fig. 2.15 Roof Longitudinal Response / Free Field Input - May 1, 1995

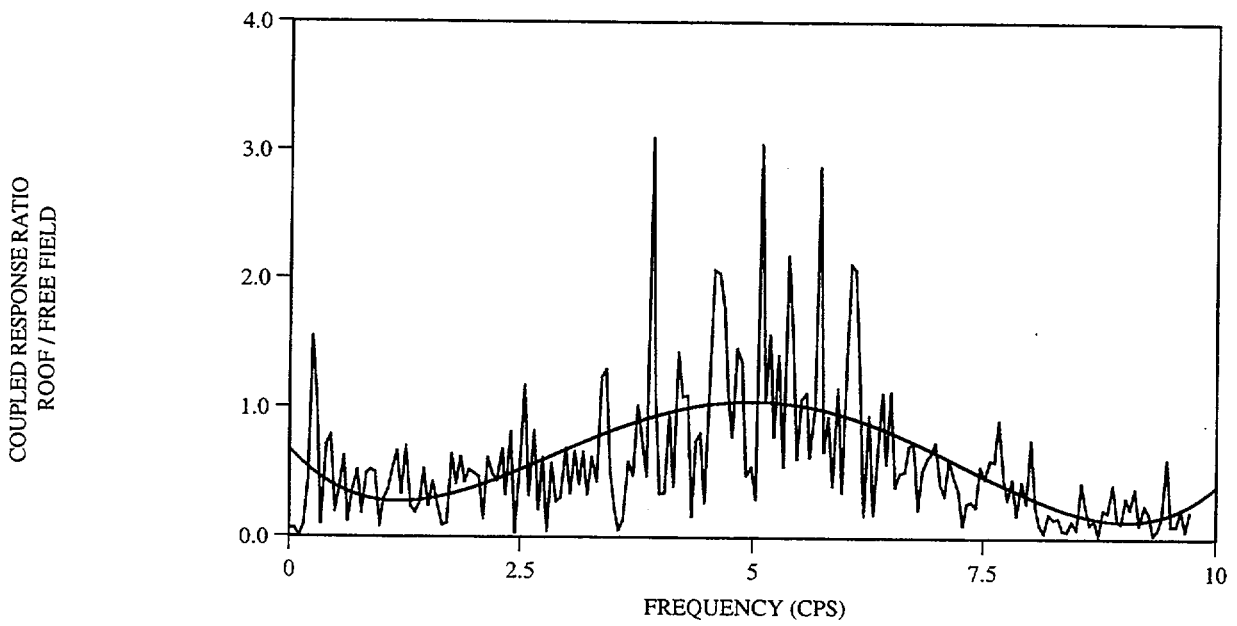


Fig. 2.16 Roof Coupled Response / Free Field Input - May 1, 1995

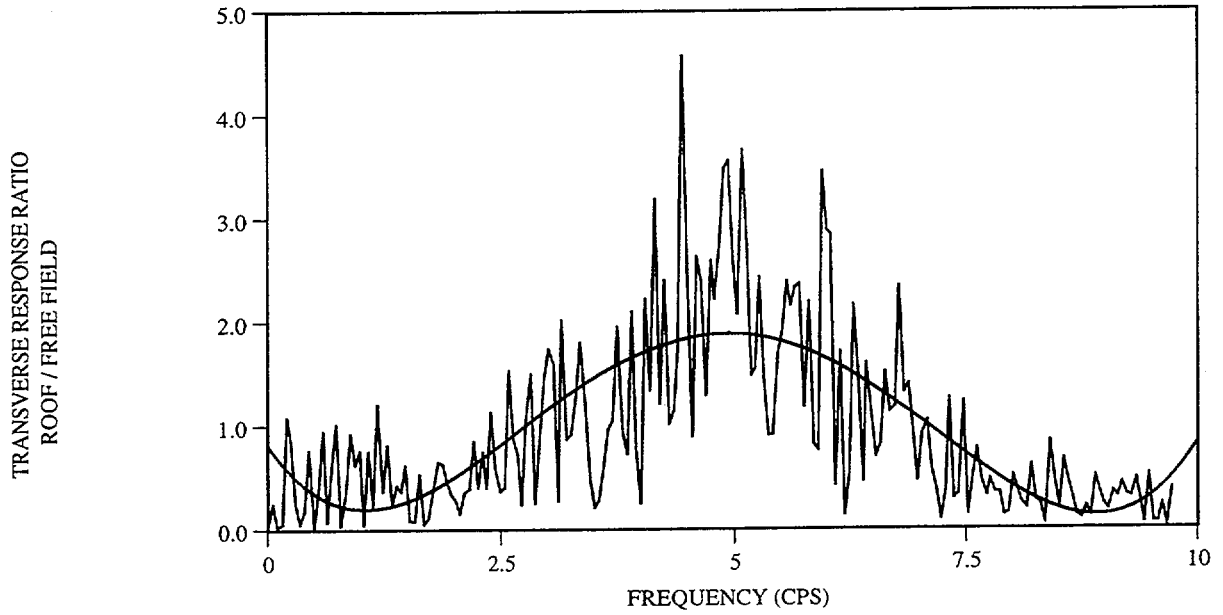


Fig. 2.17 Roof Transverse Response / Free Field Input - May 1, 1995

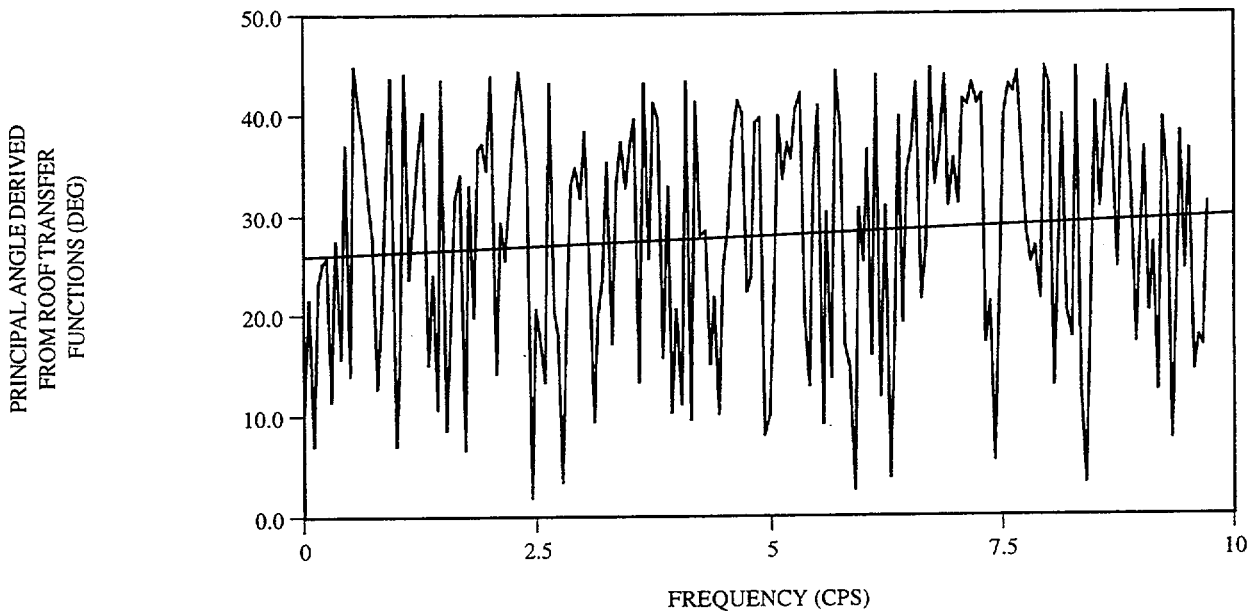


Fig. 2.18 Principal Angle Derived From Roof Data - May 1, 1995

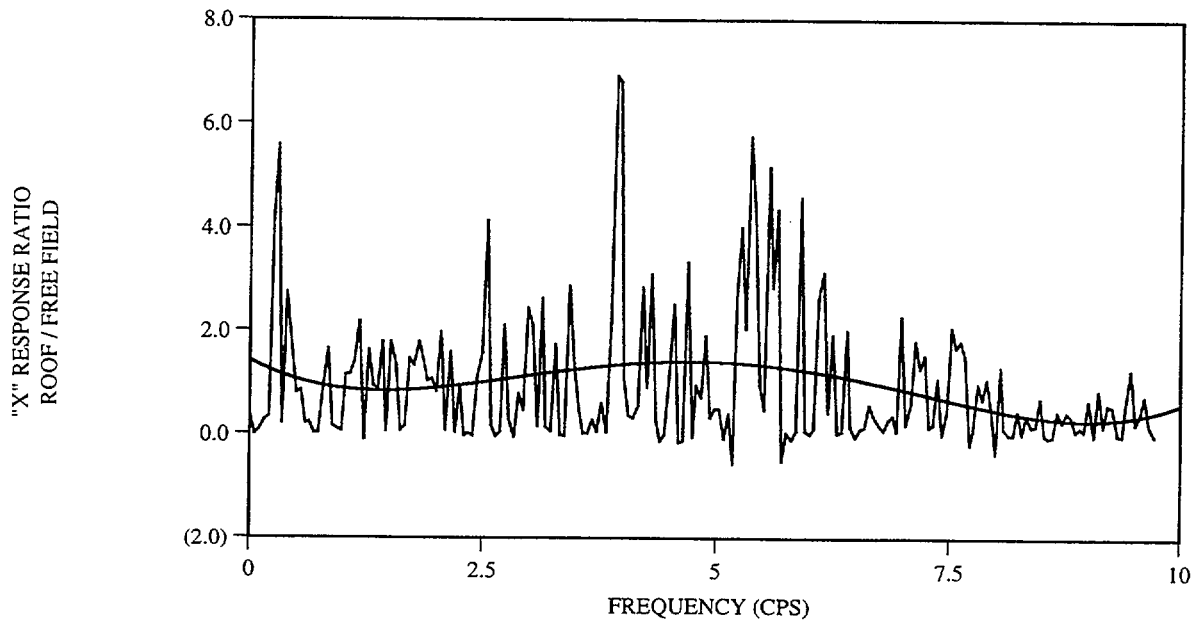


Fig. 2.19 Roof "X" Response / Free Field Input - May 1, 1995

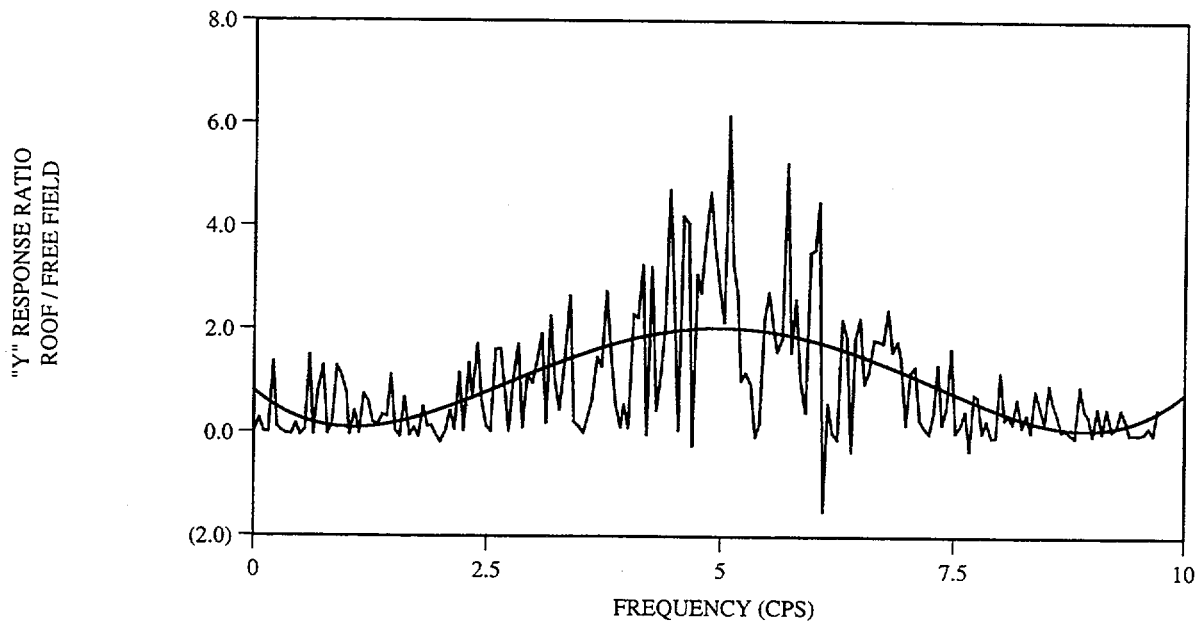


Fig. 2.20 Roof "Y" Response / Free Field Input - May 1, 1995

3.0 Measured Data

The measured data is used to evaluate characteristics of the site that may be useful in interpretation of the correlation studies. Transfer functions are developed from the measured data between various stations in the downhole array and between the model roof gages and the surface free field stations. The transfer functions are developed in both the L-T (used for the measurements) and the X-Y (principal directions as discussed in the previous section) coordinate systems. The amplitudes of the transfer functions are used in this analysis.

3.1 Transfer Functions Between Stations in the Downhole Array

Transfer functions between the gages under gage a25 are shown on Figures 3.1 through 3.4. for the February earthquake. The transfer functions obtained using the data transformed to the principal X-Y directions are shown in bold lines while the standard weight lines show the transfer functions in the L-T coordinate system. A summary of the peak amplitude and frequency at which the peak occurs is shown on Table 3.1. It is clear from these data that the transfer functions depend

Table 3.1

Characteristics of Soil Column Transfer Functions (2-23-95)

Gages	L		T		X		Y	
	Freq	Ampl	Freq	Ampl	Freq	Ampl	Freq	Ampl
d25/d26	5.0	3.4	4.4	4.9	3.4	5.5	5.4	5.2
d26/d27	3.5	4.5	2.5	2.8	2.7	4.1	3.9	5.8
d27/d28	5.0	3.4	4.4	4.9	3.4	5.5	5.4	5.2

on the orientation. This dependency continues down to the deepest gages (d27/d28) indicating that the entire site must be anisotropic. Note that the L direction is stiffer than the T direction and that the Y direction is stiffer than the X direction. Also observe that the Y stiffness is larger than the L stiffness and the X stiffness is smaller than the T stiffness. This would be expected if the site were anisotropic and the X-Y coordinate system represented the principal directions. It is also interesting to observe that there is a relatively soft layer of soil between gages d26 and d27 (the separation between gages d25 and d26 is the same as the separation between gages d26 and d27).

Estimates of average shear velocity (V_s) and ratio of critical damping (ζ) can be made from these data using the following relationships:

$$V_s = 4 H f$$

$$z = 1 / (2 A)$$

where, f = the frequency on Table 3.1

A = the amplification on Table 3.1

H = vertical separation of gages

These equations are used to develop the estimates shown on Table 3.2.

Table 3.2

Estimates of Shear Velocity (fps) and Damping(%) (2-23-95)

Gages	H (ft)	L		T		X		Y	
		V_s	ζ	V_s	ζ	V_s	ζ	V_s	ζ
d25/d26	35.4	708	15	623	10	481	9	765	10
d26/d27	35.4	496	11	354	18	382	12	552	9
d27/d28	88.6	1772	15	1559	10	1205	9	1914	10

Gage d25 is at a depth of 17.7'. The unified model specifies the low strain shear velocity to be 1040 fps between depths of 16.4' and 39.4' and 1561 fps below 39.4'. The above estimates clearly indicate lower shear velocities than those specified in the unified model. Perhaps more importantly the measured data indicate a soft zone located between a depth of 51.8' and 86.3'. The damping values also appear to be larger than indicated by the unified model.

The transfer functions between the gages under a25 for the May 1, 1995 earthquake are shown on Figures 3.5 through 3.8. There is an apparent problem with the d25T and d26T results as indicated by the unit transfer function between the two sets of data. A summary of the peak amplitude and frequency at which the peak occurs is shown on Table 3.3. It is clear from these data that the transfer functions depend on orientation. It may be seen that the frequencies are generally lower than found for the February earthquake (see Table 3.1) and the amplitudes are generally lower than for the February earthquake. This implies lower shear velocities and higher

damping in the soil for the May earthquake than was found for the February earthquake. This would be consistent with the higher shear strains found in the soil for the May earthquake.

Table 3.3

Characteristics of Soil Column Transfer Functions (5-1-95)

Gages	L		T		X		Y	
	Freq	Ampl	Freq	Ampl	Freq	Ampl	Freq	Ampl
d25/d26	4.8	3.8	-	-	-	-	-	-
d26/d27	3.4	2.6	2.8	4.6	2.0	5.5	3.2	4.4
d27/d28	2.5	5.9	1.5	3.3	1.3	3.9	1.7	2.4

3.2 Transfer Functions Between the Model and Free Field

Transfer functions are also developed between the model roof response and the surface free field input. These transfer functions are derived in both the L-T and the X-Y coordinate systems. The free field surface gages at the ends of the three arms (a15, a25, and a35) are used to define the input free field motion.

The amplitudes of the 2-23-95 transfer functions are shown on Figures 3.9 through 3.12 respectively for directions L, T, X, and Y. The L direction transfer functions (Figure 3.9) indicate fundamental frequencies of 4.3 cps, 4.9 cps, and 5.1 cps depending on whether gage a15, a25, or a35 is used to represent the free field. It is also interesting to recall that the fundamental frequency of the model as found from the forced vibration tests (see volume 3) was about 6 cps. The picture is even more complex when the T direction transfer functions shown on Figure 3.10 are examined. The peaks of these transfer functions occur over a much broader frequency range from about 3 cps to 6 cps and also show a significant variation depending on the reference gage used for the free field. The primary response found in the forced vibration tests was the rigid body rocking mode with relatively small contributions from the flexural and rigid body translation modes. One would expect narrow banded transfer functions for this type of problem rather than the wide band results observed in the T direction functions. Both the dependency of the transfer functions on the location of the free field gage used to define the input motion and the difference in the L and T direction transfer functions are likely caused by anisotropic site effects. These anomalies between the

observed data and the expected behavior indicate that one should expect poor correlation between the measured and computed results.

The transfer functions in the principal X-Y directions (Figures 3.11 and 3.12) show similar characteristics. This indicates that a simple transformation of the measured data to the principal directions is not likely to improve the correlation between the measured and computed results.

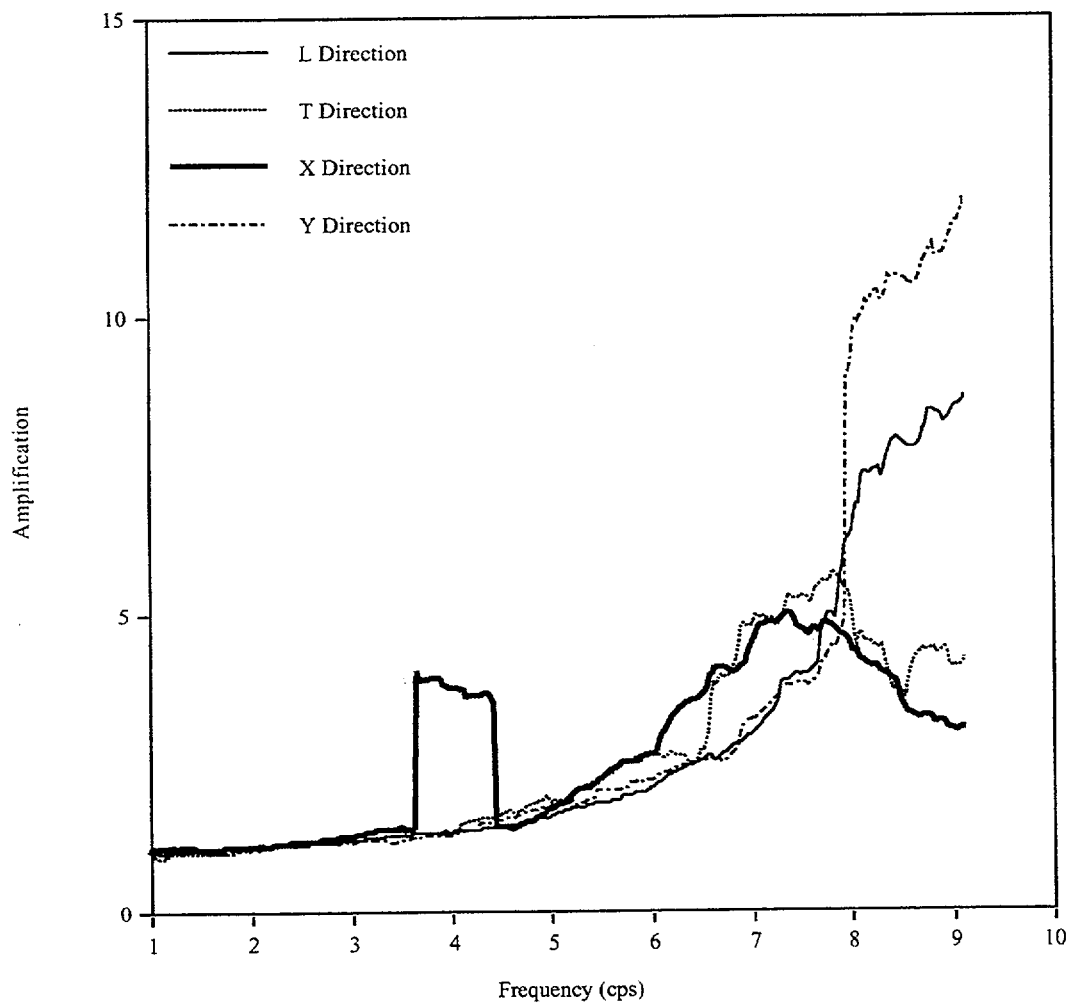


Fig. 3.1 Transfer Functions a25/d25; 2-23-95

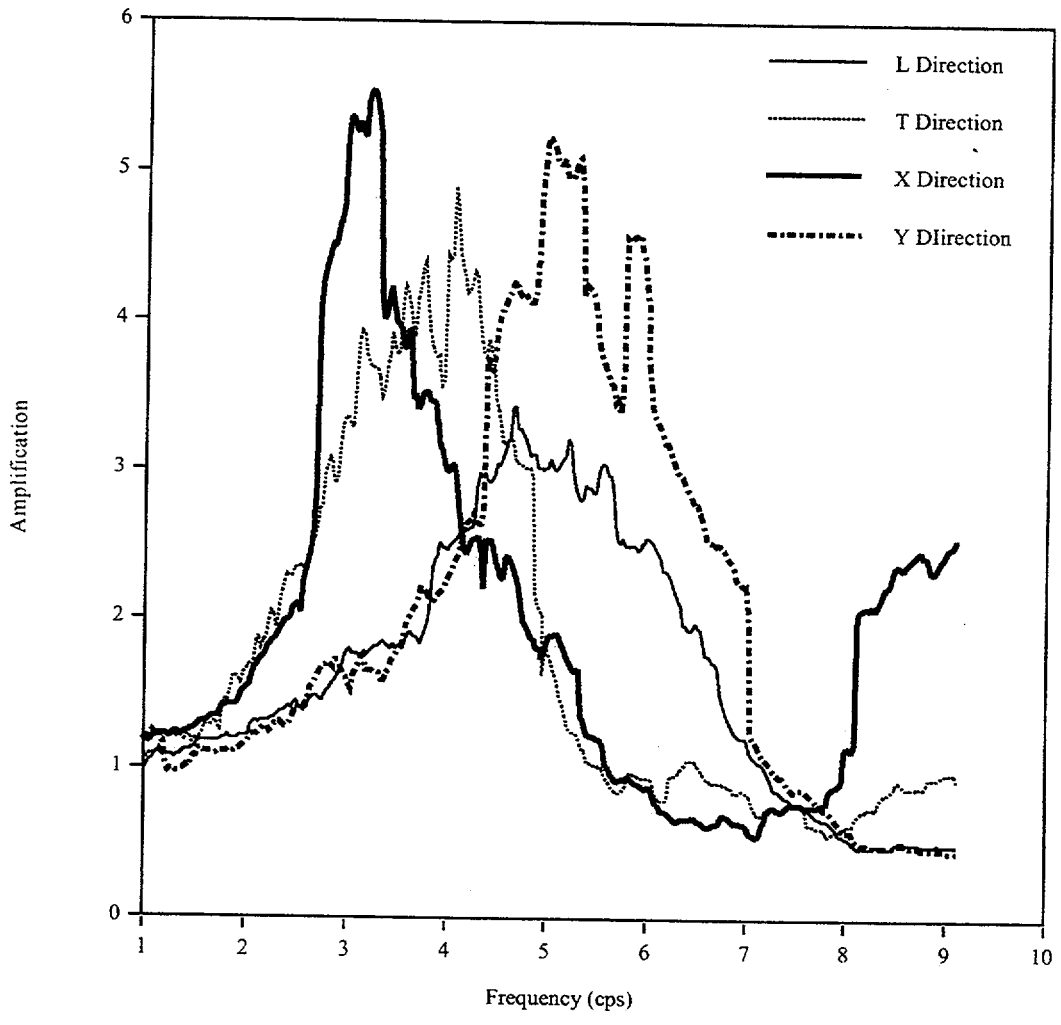


Fig. 3.2 Transfer Functions d25/d26; 2-23-95

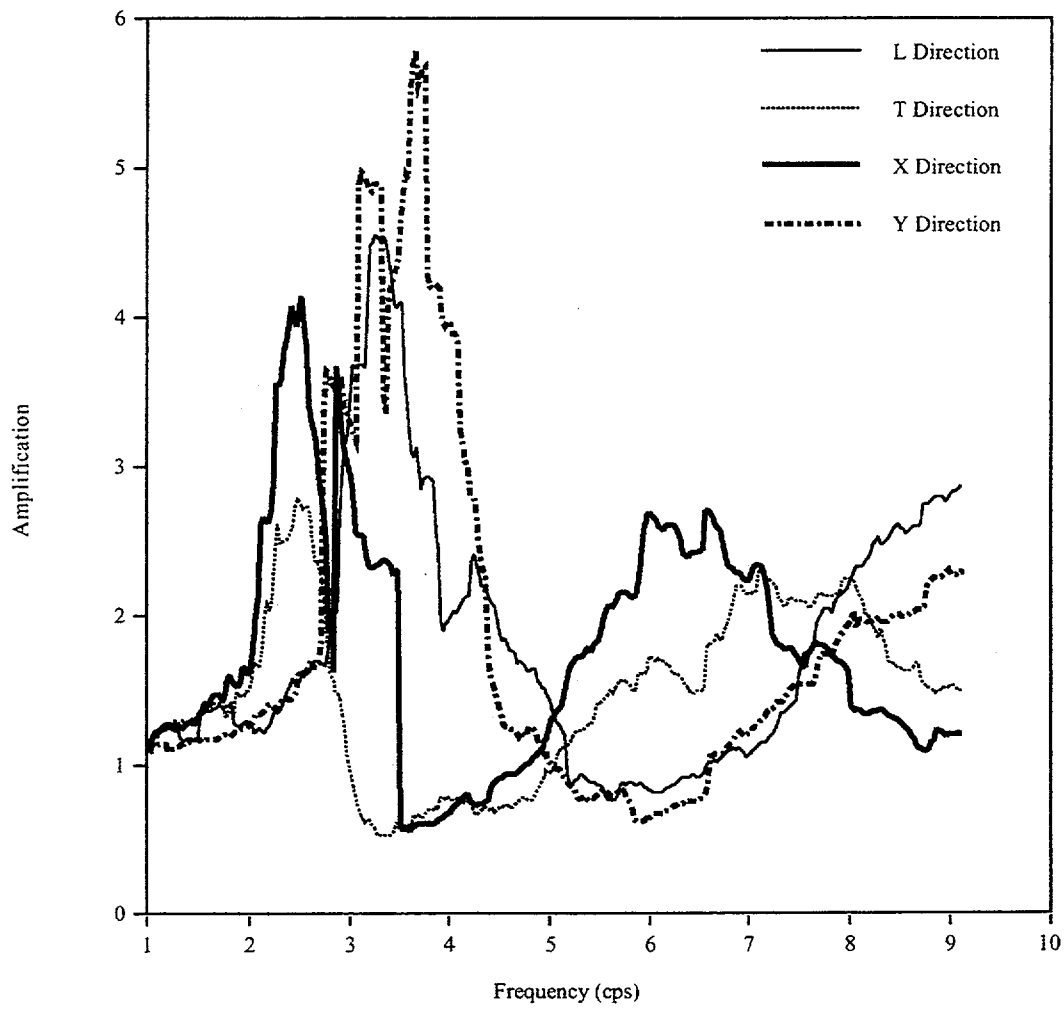


Fig. 3.3 Transfer Functions d26/d27; 2-23-95

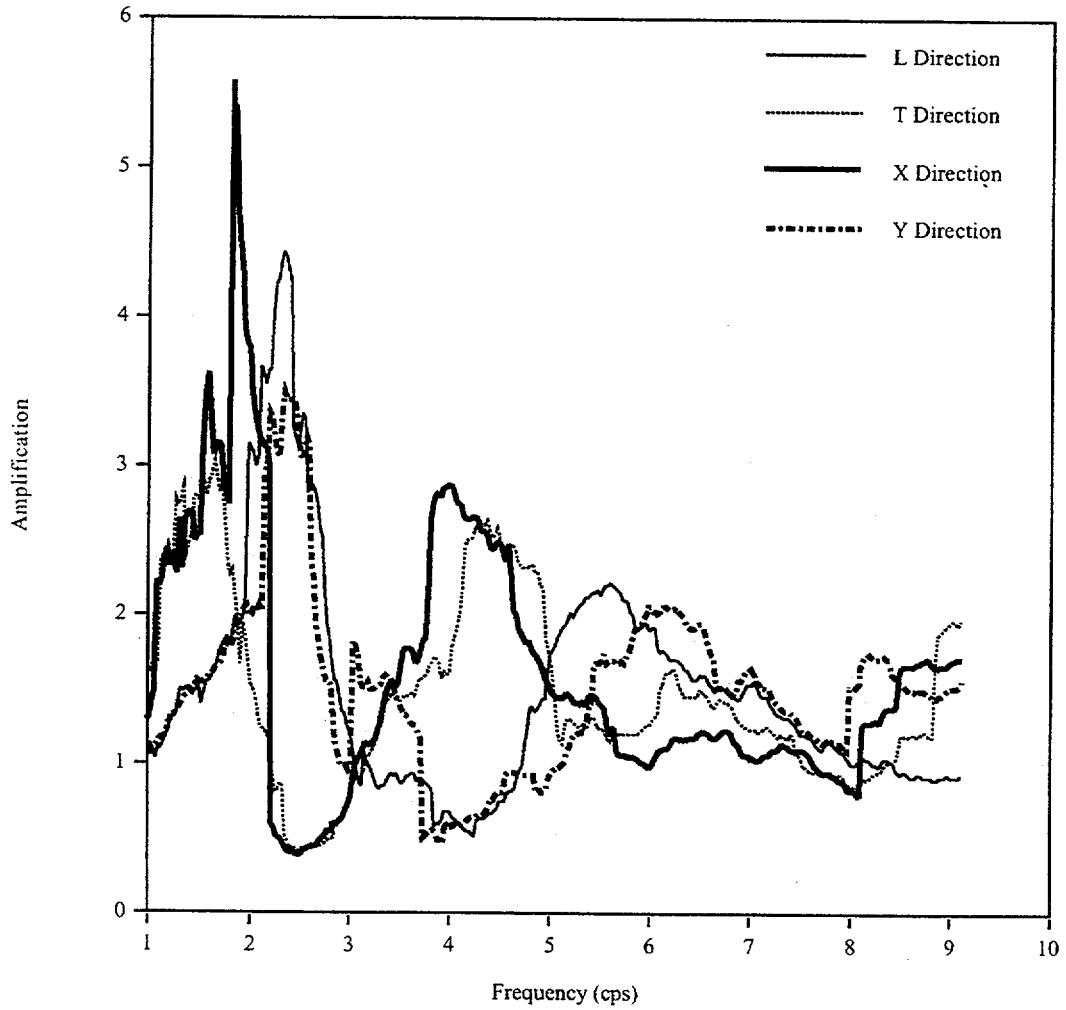


Fig. 3.4 Transfer Functions d27/d28; 2-23-95

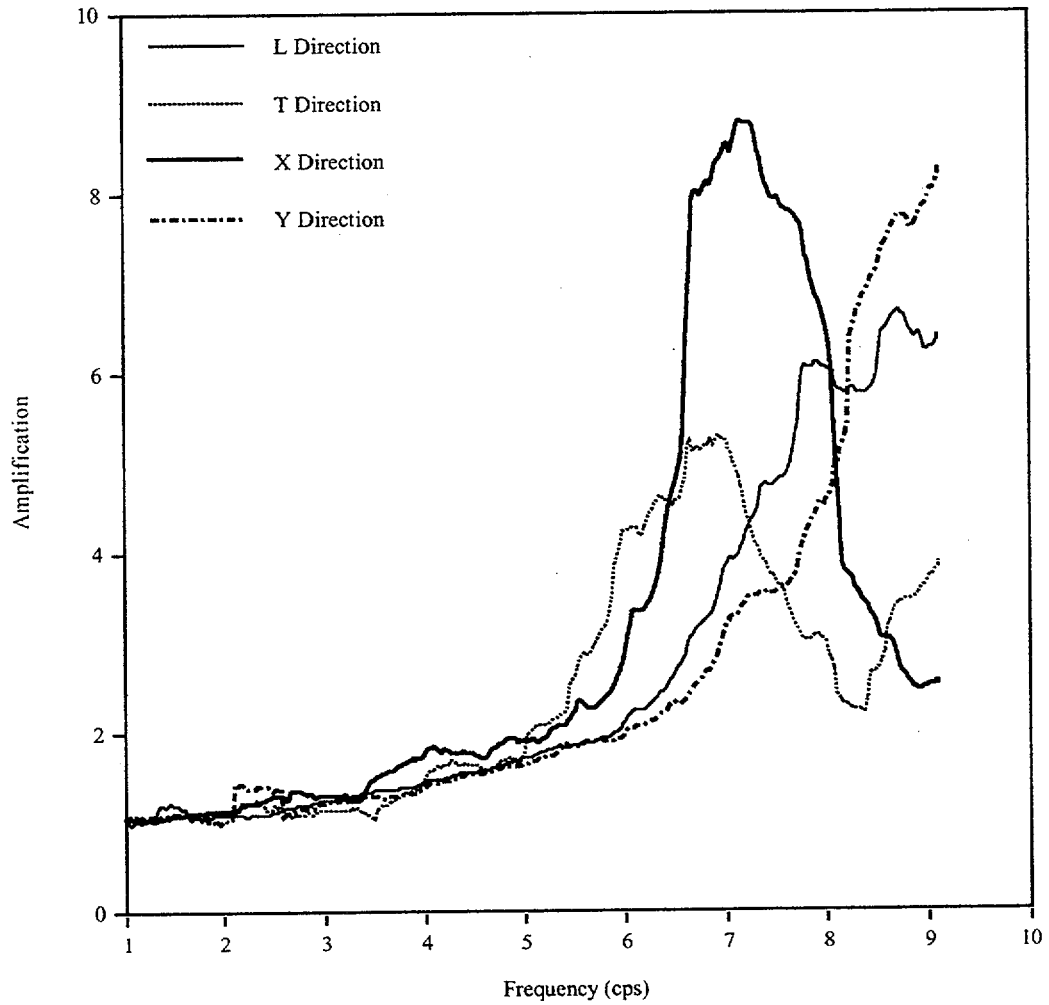


Fig. 3.5 Transfer Functions a25/d25 - 5-1-95

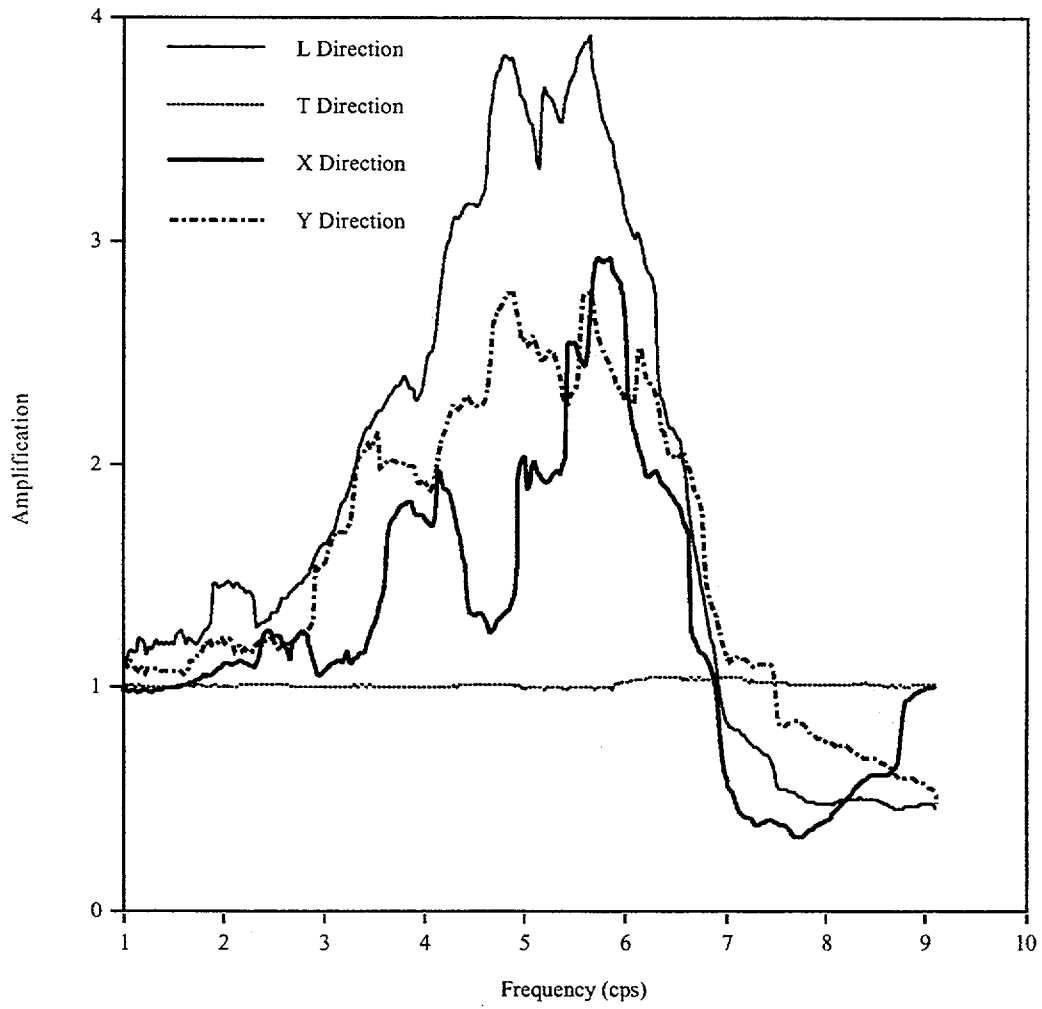


Fig. 3.6 Transfer Functions d25/d26; 5-1-95

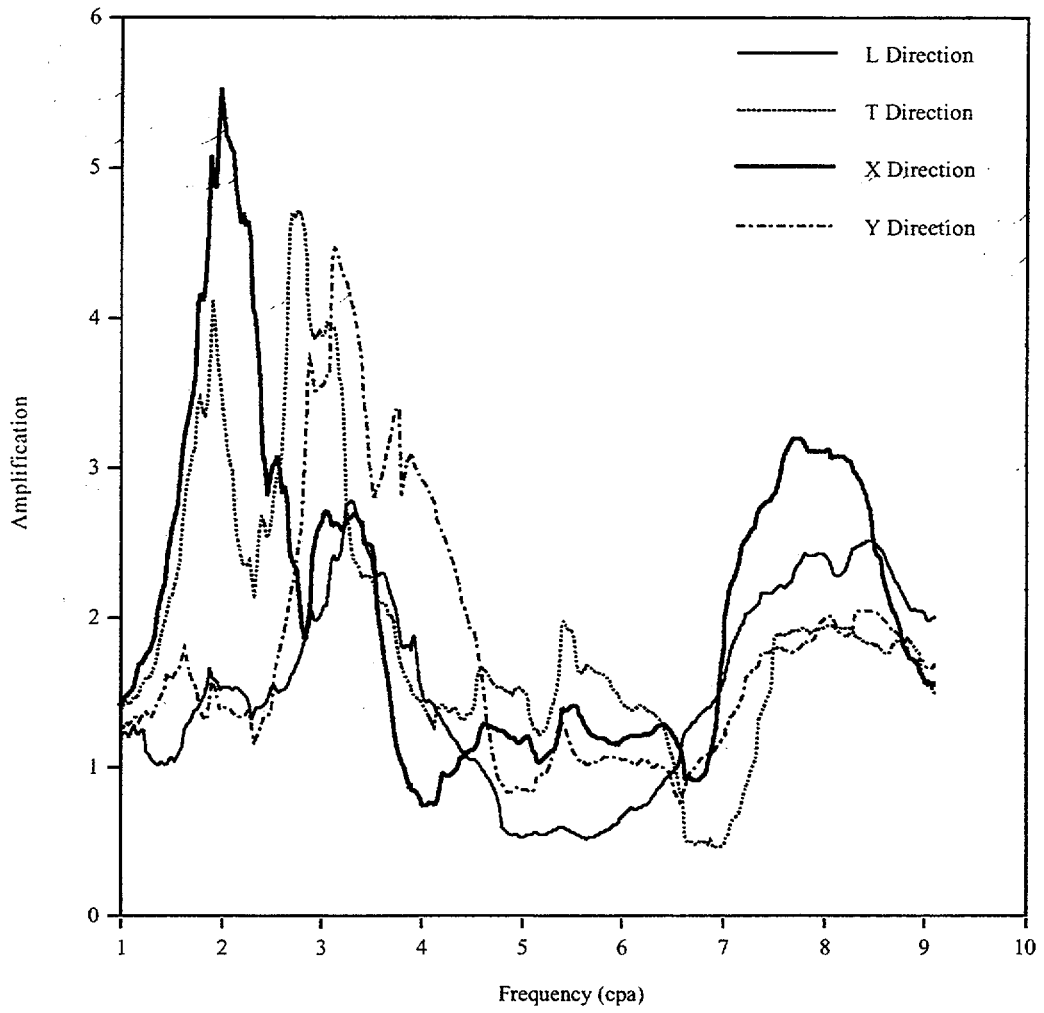


Fig. 3.7 Transfer Functions d26/d27; 5-1-95

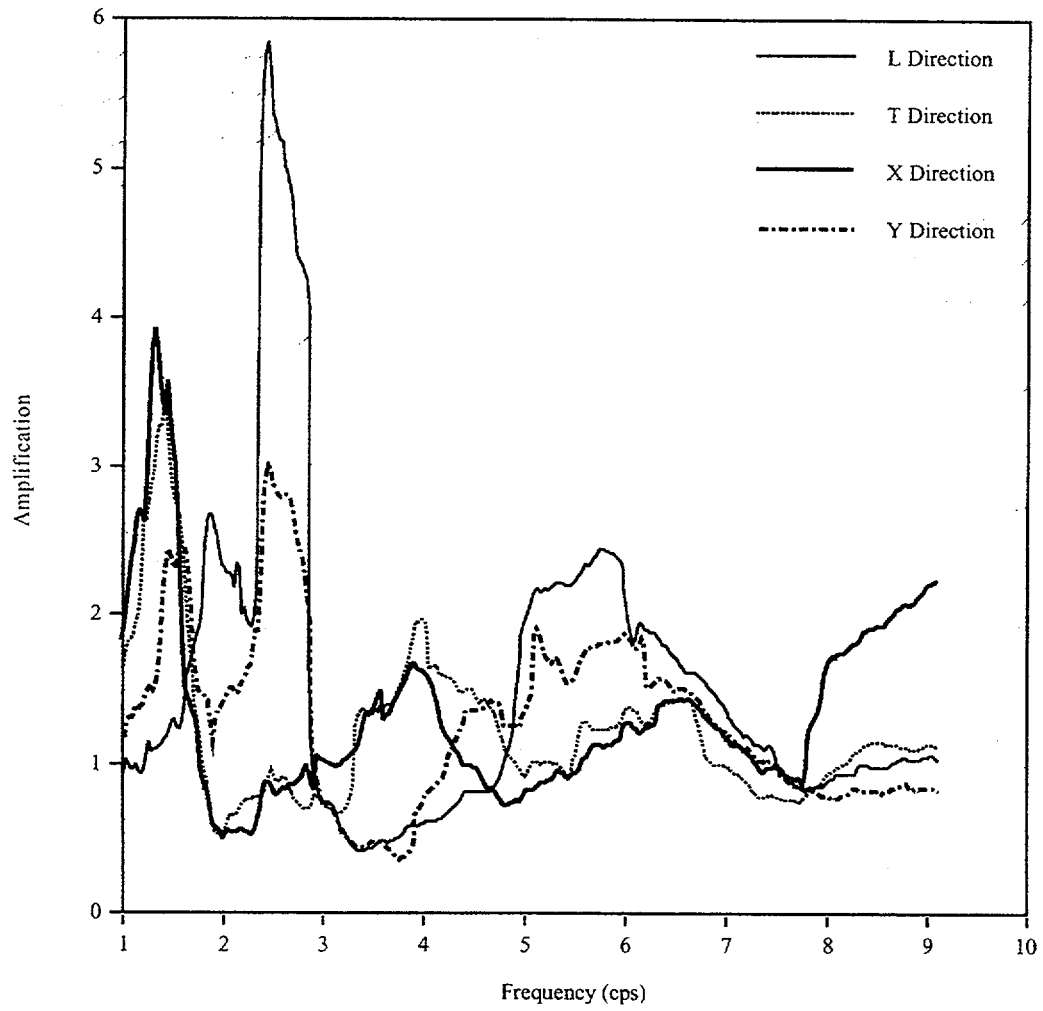


Fig. 3.8 Transfer Functions d27/d28; 5-1-95

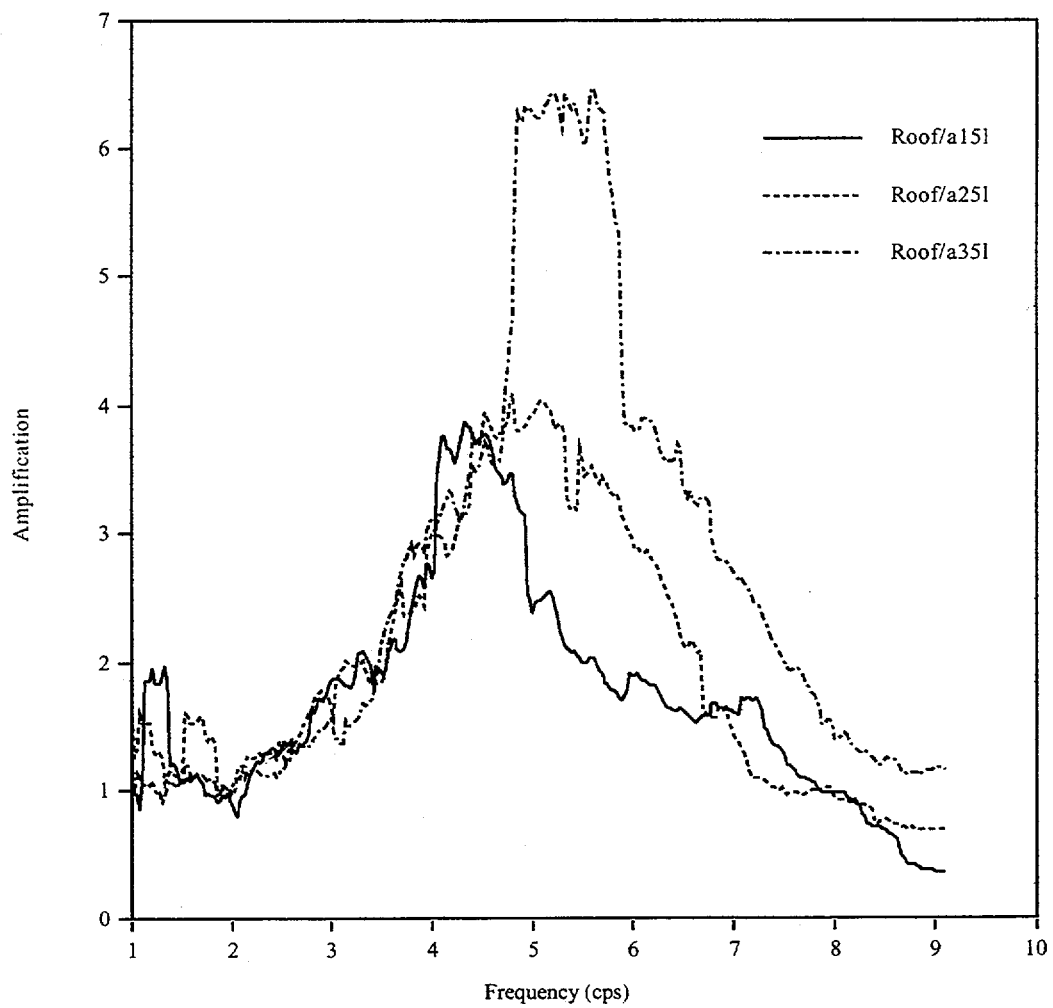


Fig. 3.9 L Transfer Functions Between Roof and Furthest Free Field Gages; 2-23-95

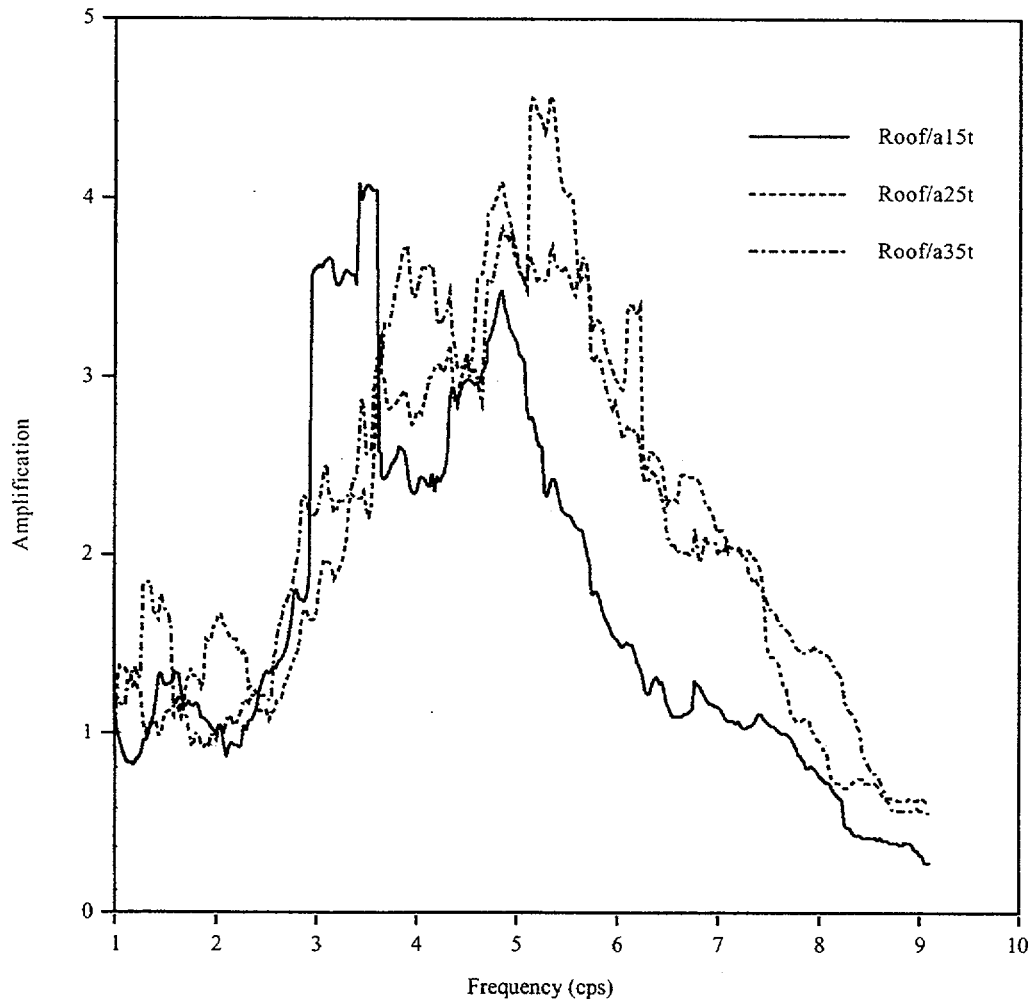


Fig. 3.10 T Transfer Functions Between Roof and Furthest Free Field Gages; 2-23-95

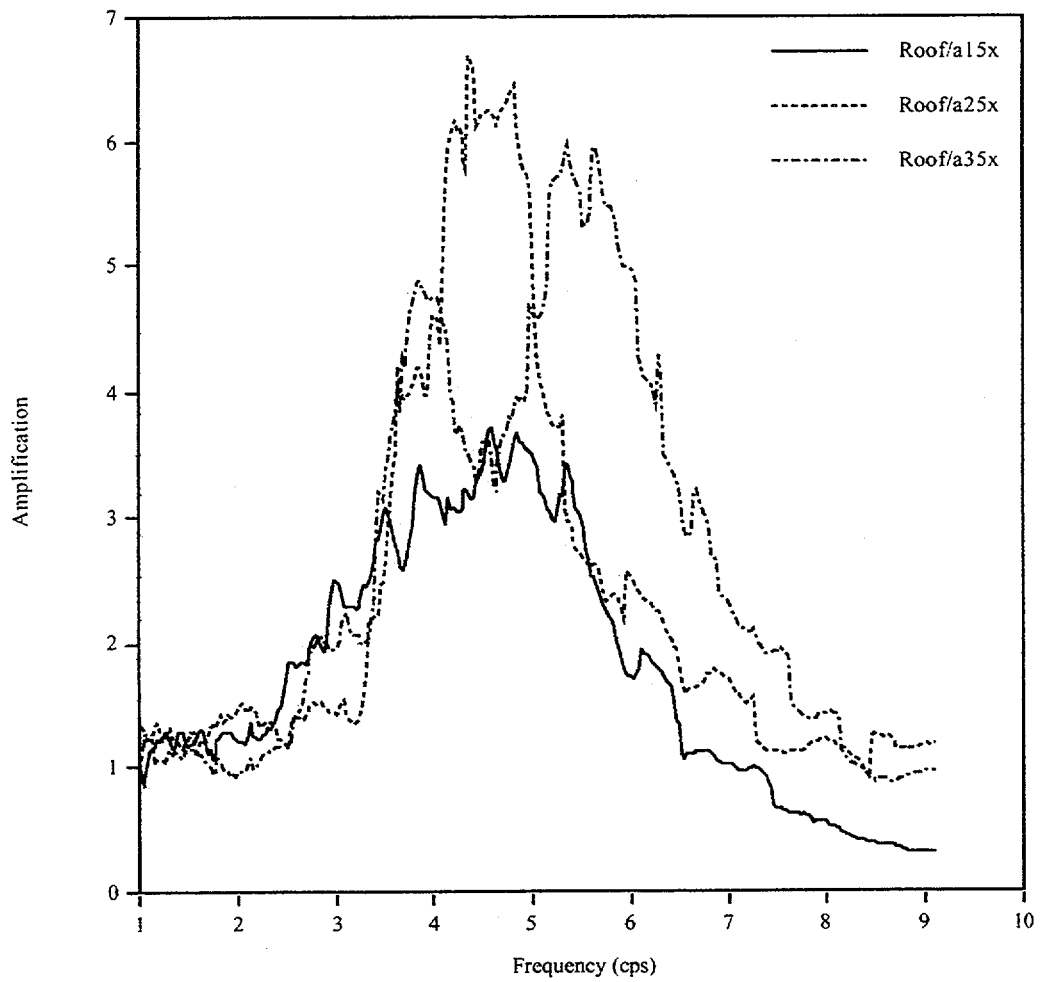


Fig. 3.11 X Transfer Functions Between Roof and Furthest Free Field Gages; 2-23-95

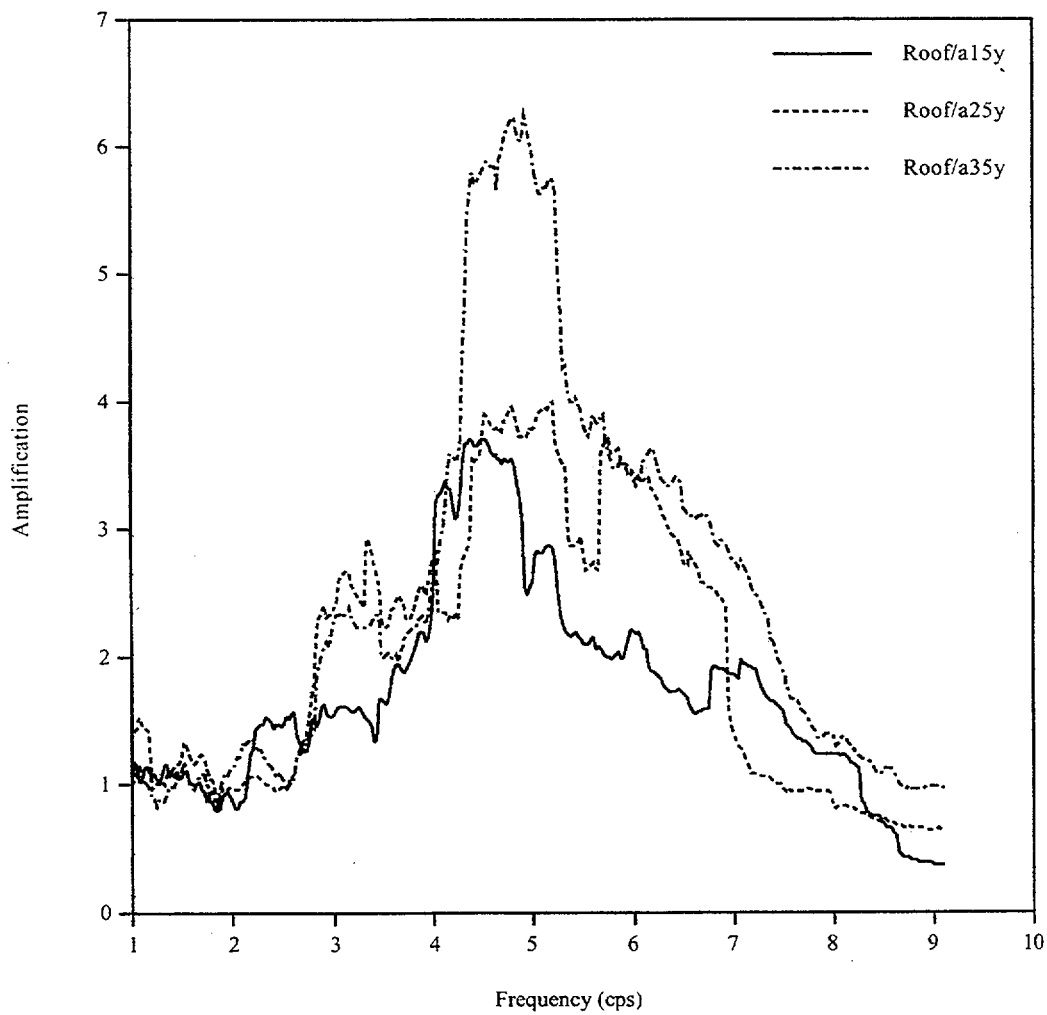


Fig. 3.12 Y Transfer Functions Between Roof and Furthest Free Field Gages; 2-23-95

4.0 Correlation of Predicted with Measured Free Field Response

Deconvolution studies are performed for the downhole gages located under gage a25 (see Figure 2.2). The gage is located at the end of ARM 2 and is 5 diameters from the center of the model. The surface motion at a25 is deconvolved to the depths of the "d" gages assuming vertically propagating, horizontally polarized shear waves for the horizontal components and vertically propagating compression waves for the vertical motion. The CARES computer code is used to perform these deconvolution studies for motions in the X, Y, and vertical (V) directions. These studies are performed for both the February 23, 1995 and May 1, 1995 earthquakes.

The soil properties shown on Figure 2.1 and located outside of the backfill area are specified as the low strain properties of the soil column with the CRIEPI degradation characteristics used to account for strain dependency of the soil properties. The model used for the convolution studies in both the horizontal X Y directions is shown on Figure 4.1. The solution is carried out in an iterative fashion with the soil properties modified at each iteration to account for shear modulus degradation and soil damping increase as a function of soil strain. Since the soil is saturated the compressional wave velocity used for the vertical motion is limited to that of water (5,500 fps). No degradation is included in the vertical motion studies.

The peak shear strains found for the horizontal response during the February 1995 earthquake are shown on Table 4.1. The maximum shear strain found for the convolution studies in the horizontal directions are 0.0044% and 0.0023 % for the X and Y direction studies respectively. The average shear strains over the depth of the soil column are about 0.0030 % and .0015 % for the two directions. These average shear strains result in shear moduli values equal to about 90 % of the low strain values and damping equal to about 2.5% (the low strain damping is 2 %). It can be seen that the strains are not high enough to have a significant effect on the soil properties.

A comparison of response spectra based on the measured and computed X and Y free field motions is shown on Figures 4.2 and 4.3 for gages d25 (5.3 m), d26 (15.8 m), d27 (26.3 m), and d28 (52 m). The predicted values are essentially identical to the measured data over the depth of the model (gage d25), and reasonably good comparisons are found down to depths of 52 m. The correlations are somewhat better in the Y than the X direction. It is interesting to note that the primary energy content of the earthquake (see spectra of measured data at gage d28 on the figures) is at 3 cps for the X component and less than 2 cps for the Y component. Average column frequencies can be determined from $(V_s/4H)$. If this is used the frequencies of the columns above the four gage depths can be estimated to be about 10 cps, 5 cps, 3 cps, and 2 cps for gages d25 through d28 respectively. The column frequencies at gages d26 and d27 are close to the 3 cps of the

input motion below. Perhaps this accounts for the relatively poor correlation of measured and computed motions in the X direction at these gages. Note that the disagreement occurs at frequencies of 2 - 4 cps. This disagreement indicates that perhaps the soil damping used in the model is too large. It should be noted that convolution studies performed in the L, T rather than X, Y coordinates resulted in good results in the L direction but very poor results in the T direction. This suggests again that the site is not isotropic and that it is important to perform correlation studies in the principal directions.

Table 4.1

Peak Shear Strains for February 1995 Earthquake

Depth (ft)	Strain (%) X Response	Strain (%) Y Response
3.28	.0018	.0011
9.02	.0014	.0009
13.94	.0021	.0014
19.27	.0011	.0007
25.01	.0015	.0010
30.75	.0020	.0013
36.49	.0025	.0016
46.41	.0014	.0009
60.51	.0017	.0011
74.61	.0021	.0013
88.71	.0026	.0015
102.81	.0030	.0017
116.91	.0033	.0019
131.01	.0036	.0020
145.11	.0039	.0022
159.21	.0039	.0022
173.31	.0044	.0023

The vertical convolution is performed using a bulk modulus that is derived from the shear velocity and Poisson's ratio shown on Figure 2.1 but the bulk modulus is restricted to give the compressional wave velocity of water). Degradation of soil properties is not considered for the vertical motion convolution studies. A comparison of spectra based on the measured and computed vertical motions is shown on Figure 4.4 for the four downhole gage locations. As may be seen excellent agreement is found at all depths except at frequencies greater than 10 cps. This is about

the frequency of the column down to the depth of the d28 gage ($\sim V_s/4H = 1645 / 4 * 52 = 8$ cps). The spectral values at lower frequencies are essentially propagated through the column with little modification. This probably accounts for the good agreement. It appears that much less damping (than the 2 %) is required in the soil model to reduce the attenuation of the vertical motion as it propagates from the 52 m depth to the surface.

The peak shear strains found for the horizontal response during the May 1, 1995 earthquake are shown on Table 4.2. The maximum shear strain found for the convolution studies in the horizontal directions are 0.0076% and 0.0045 % for the X and Y direction studies respectively. These are about double those found for the February earthquake and would result in shear moduli values equal to about 75 % of the low strain values and damping equal to about 5 % (the low strain damping is 2 %).

A comparison of the computed free field response with the measured horizontal motion (X and Y directions) data are shown on Figures 4.5 and 4.6 for the May 1, 1995 event. The comparisons are generally comparable to those found for the February event. The comparison for the vertical component is shown on Figure 4.7. The large spectral acceleration spike in the computed spectra at about 30 cps results from the larger spike in the measured surface spectra (see Figure 2.5). It is not clear why this spike does not show up in the measured data at the deeper gages.

Table 4.2

Peak Shear Strains for May 1, 1995 Earthquake

Depth (ft)	Strain (%) X Response	Strain (%) Y Response
3.28	.0031	.0050
9.02	.0024	.0038
13.94	.0039	.0052
19.27	.0022	.0027
25.01	.0031	.0032
30.75	.0042	.0039
36.49	.0050	.0048
46.41	.0027	.0024
60.51	.0033	.0028
74.61	.0040	.0032
88.71	.0047	.0036
102.81	.0054	.0040
116.91	.0060	.0043
131.01	.0066	.0043
145.11	.0072	.0044
159.21	.0073	.0044
173.31	.0076	.0045

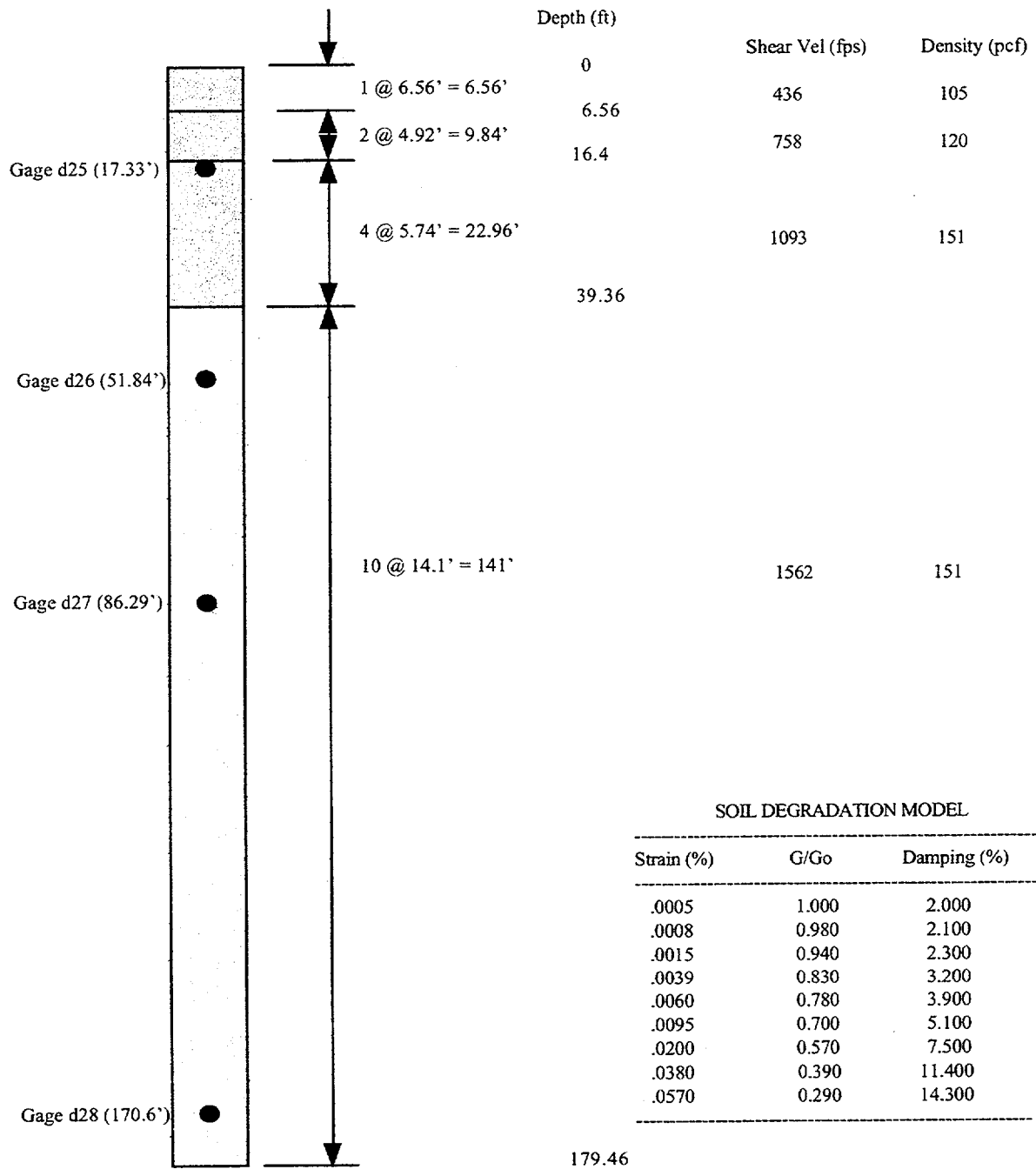


Fig. 4.1 Soil Column Model Used for Convolution Analyses

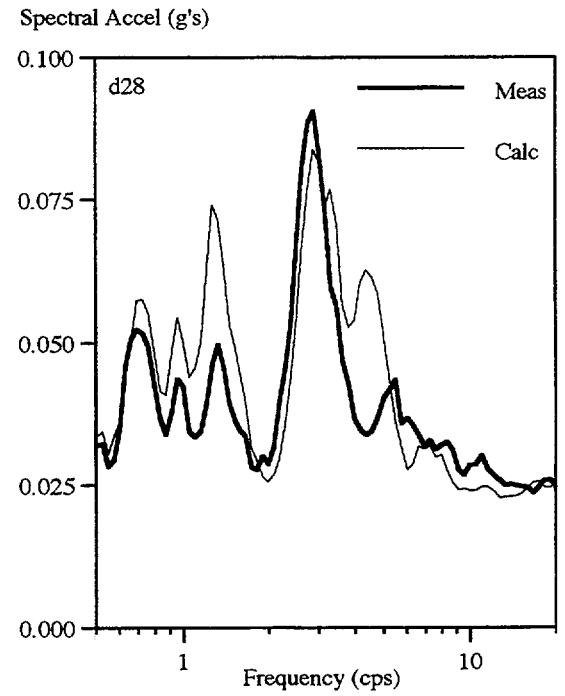
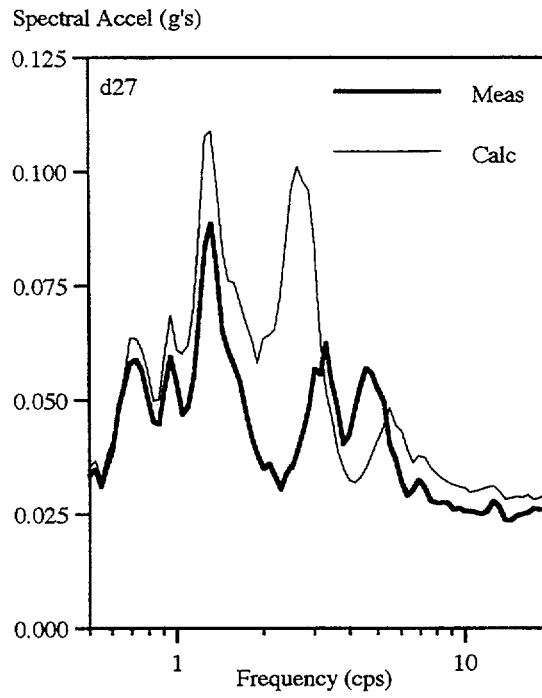
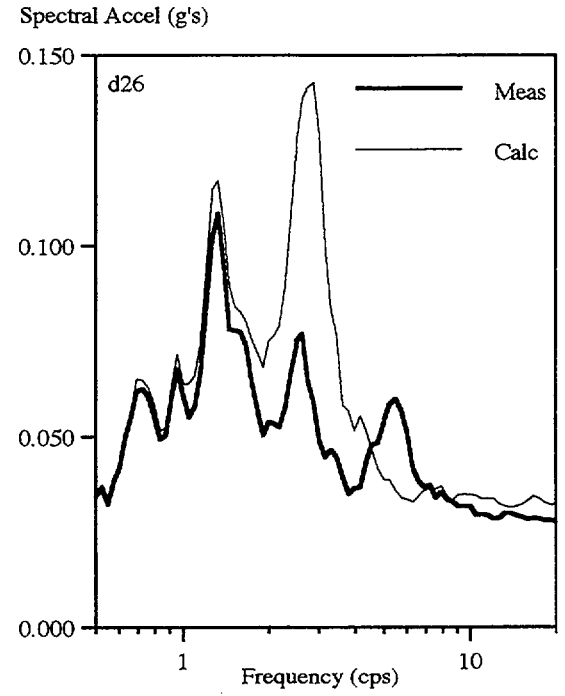
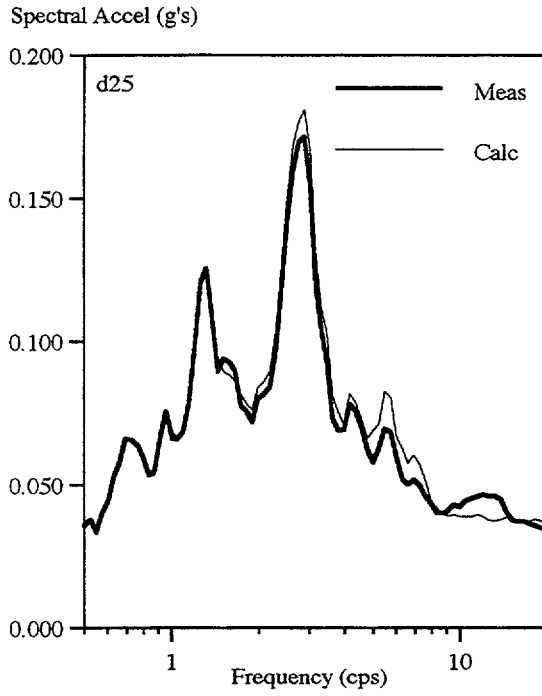


Fig. 4.2 Comparison of Computed and Measured Free Field X Spectra (5%); 2-23-95

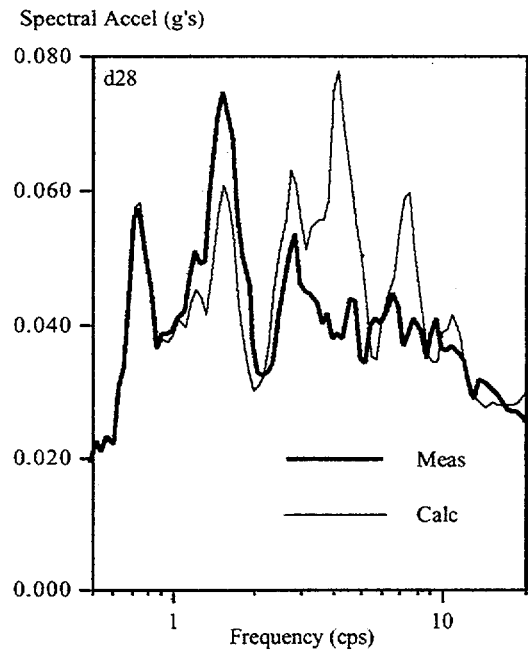
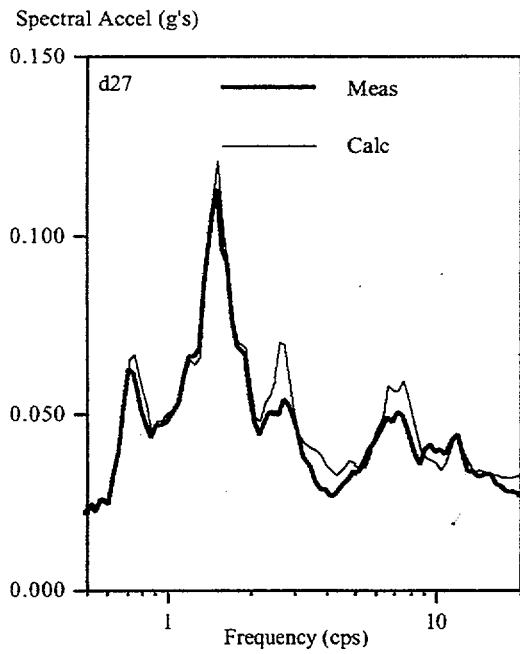
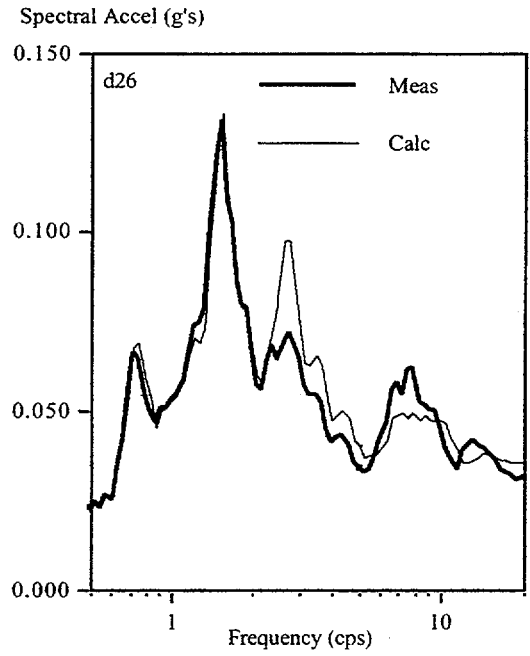
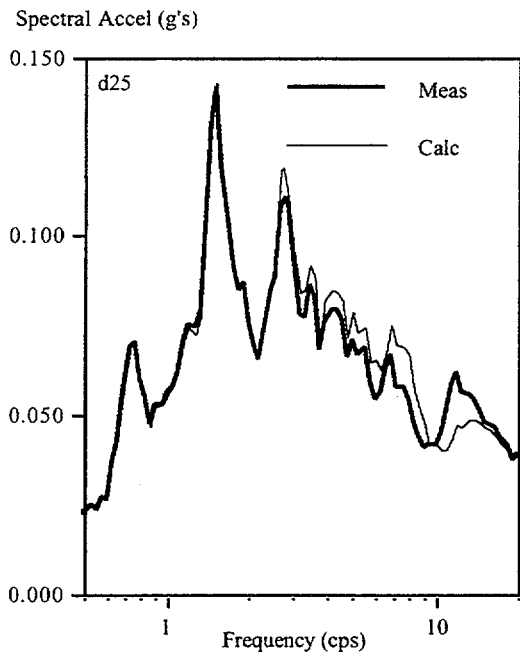


Fig. 4.3 Comparison of Computed and Measured Free Field Y Spectra (5%); 2-23-95

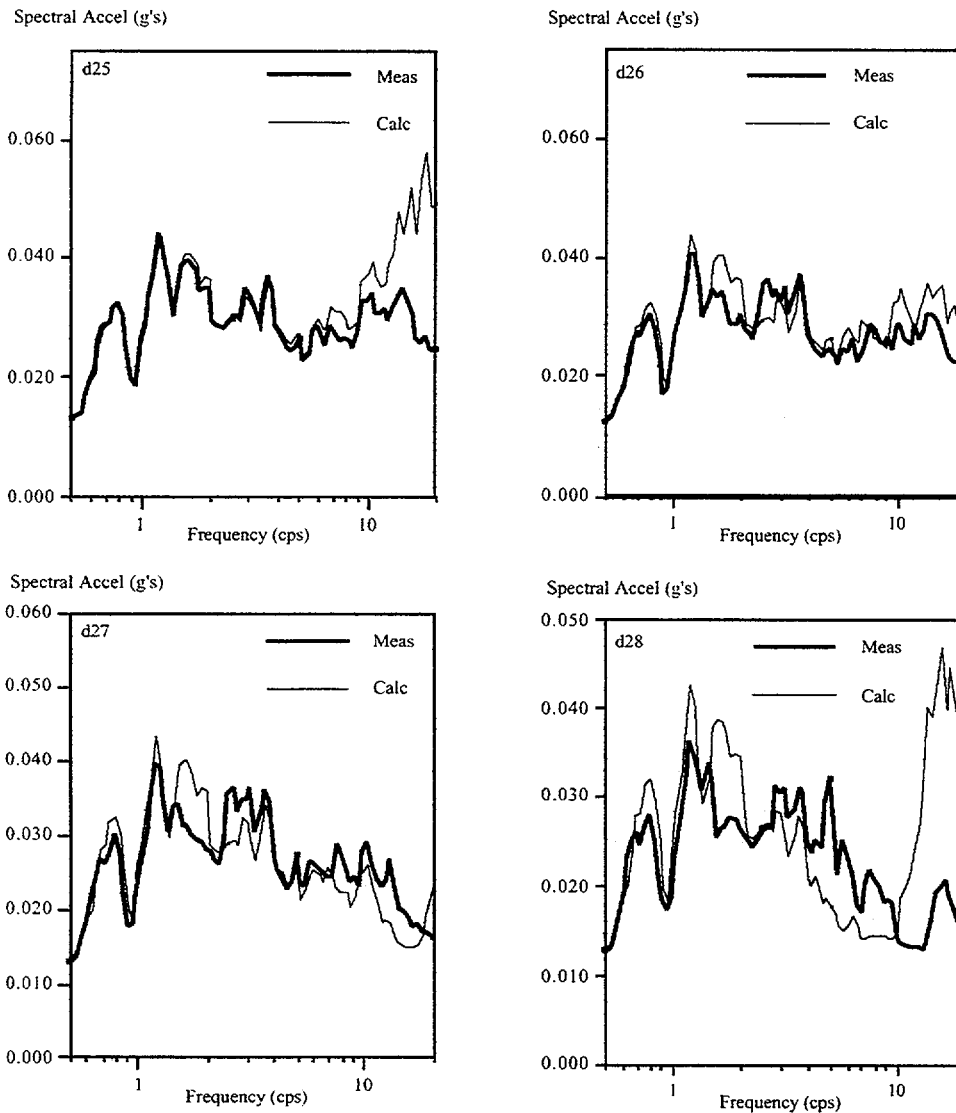


Fig. 4.4 Comparison of Computed and Measured Free Field V Spectra (5%); 2-23-95

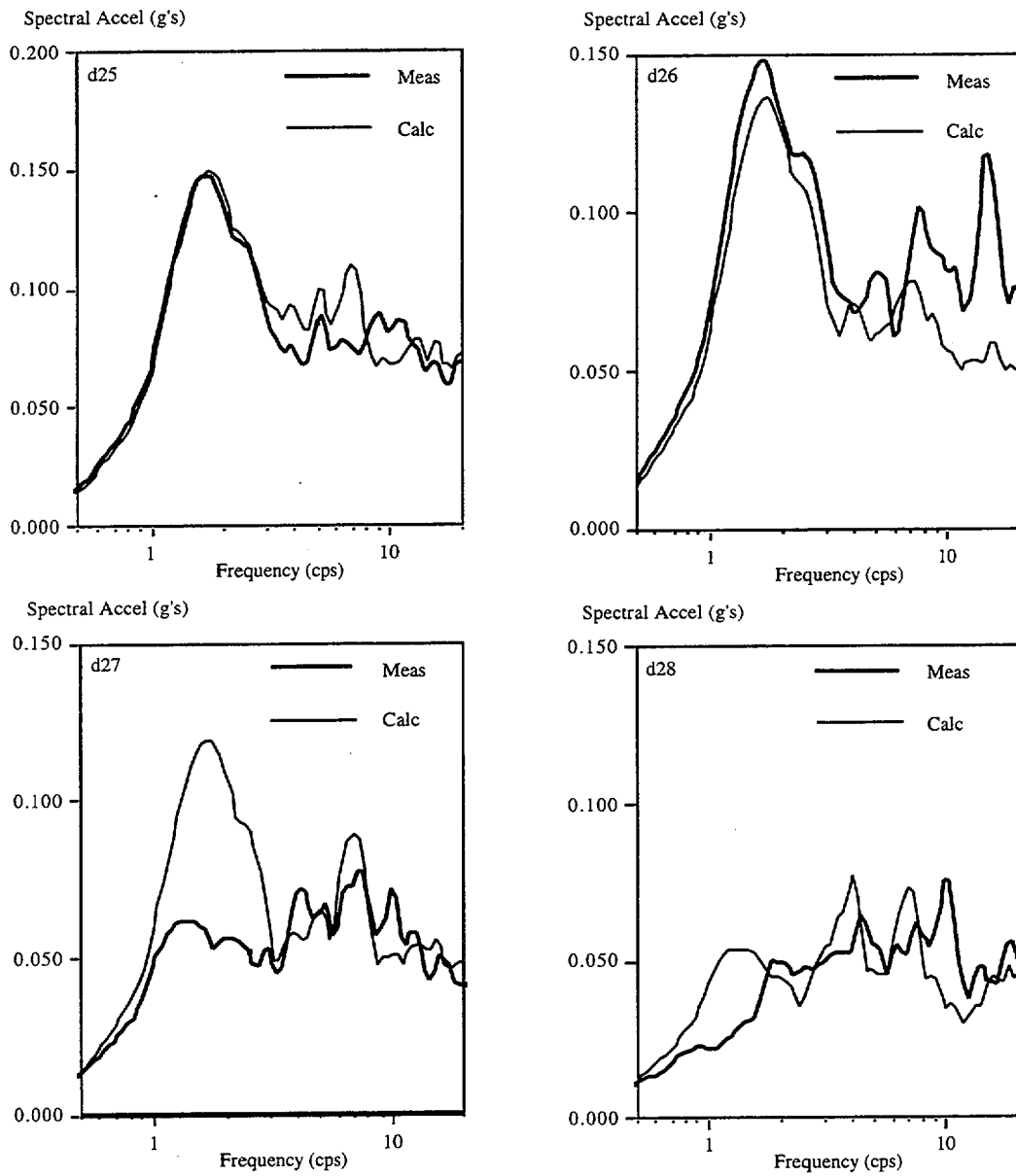


Fig. 4.5 Comparison of Computed and Measured Free Field X Spectra (5%); 5-1-95

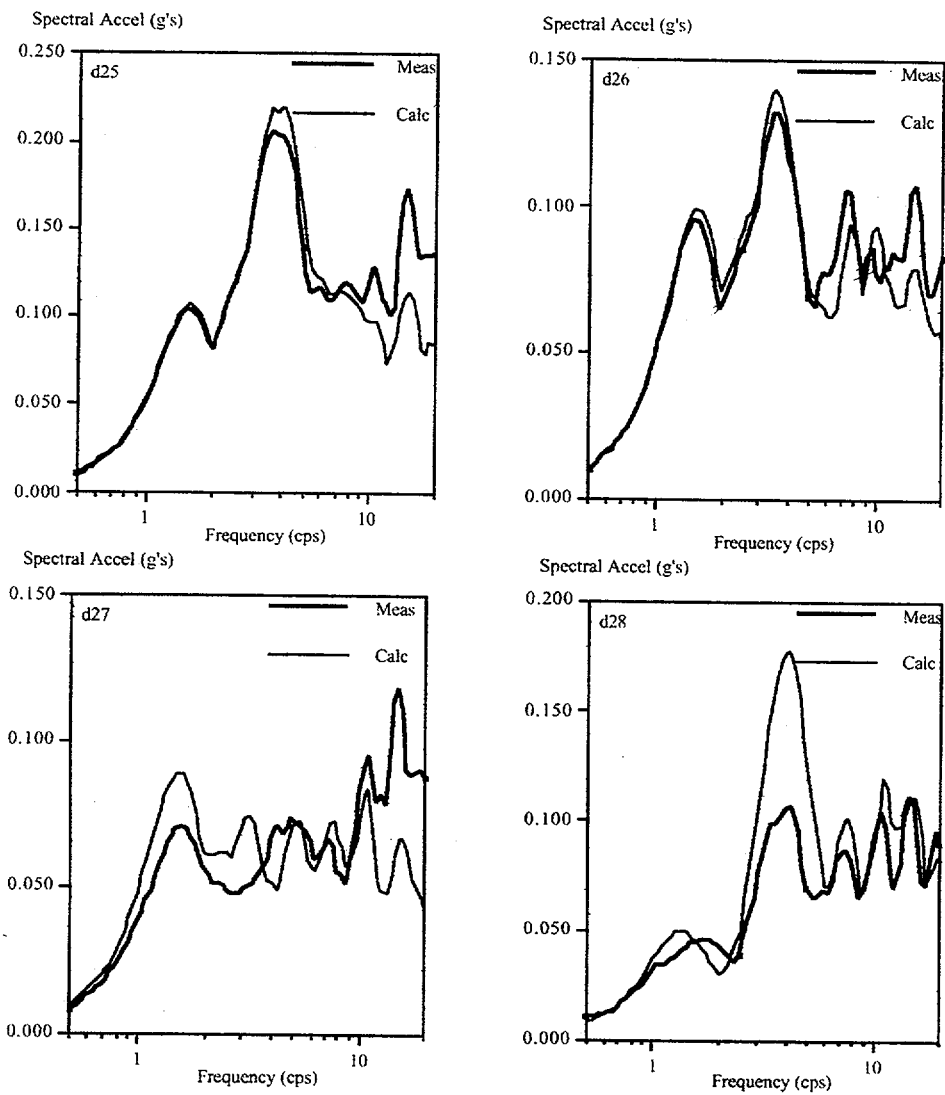


Fig. 4.6 Comparison of Computed and Measured Free Field Y Spectra (5%); 5-1-95

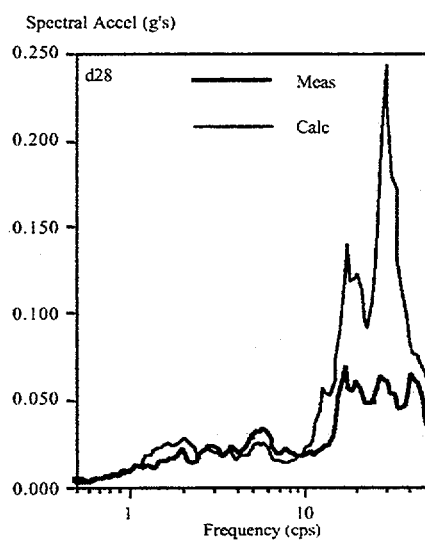
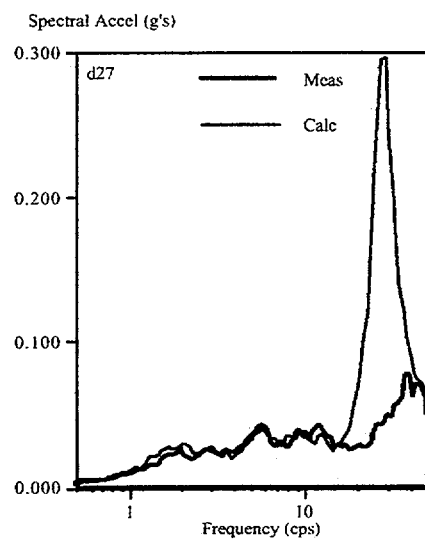
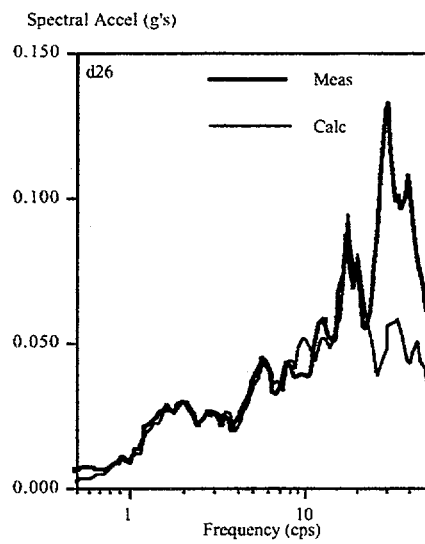
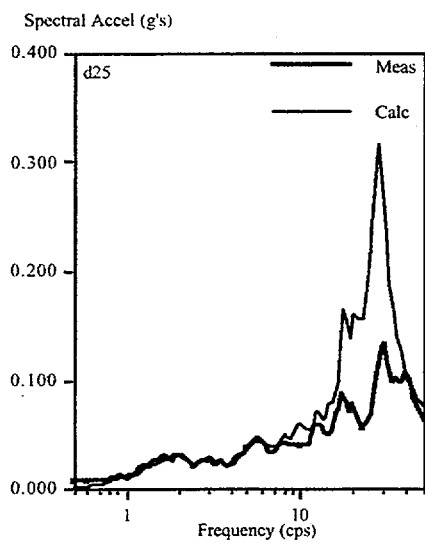


Fig. 4.7 Comparison of Computed and Measured Free Field V Spectra (5%); 5-1-95

5.0 Correlation of Predicted with Measured Model Response

Model response studies are also carried out for the February 23, 1995 and May 1, 1995 events. The measured responses (in the principal horizontal X - Y directions and the vertical direction) at the roof and basemat elevations are compared with the predicted responses.

The CARES computer program is used to make the predictions. The same structural model is used for these predictions as was used for the forced vibration predictions described in Volume 3 of this report. The cylindrical portion of the structure is modeled with three dimensional shear beams, and the roof and basemat are treated as rigid masses. Proportional structural damping equal to 2 % is used and the damping matrix is taken to be proportional to the stiffness and mass matrices. Rigid links are used to model the thickness of the roof slab and basemat and to obtain output at the gage locations on the structure.

Soil structure interaction effects are treated with the Beredugo - Novak frequency dependent model as included in CARES. This model allows for separate properties of the soil beneath the foundation and to the side of the foundation. The shear modulus of the soil beneath the foundation is obtained as the average of the moduli in the soil from the foundation to a depth of 40'. The side soil shear modulus is determined based on the in-situ material (rather than the backfill) with a weighted average computed for the layers based on the rocking response mode. In both cases the degraded moduli as found from the convolution studies (see Section 4) are used for the model response evaluations. The measured free field motion at gage a25 is used as input to the model. Kinematic interaction effects are not included in the results.

The soil properties used for the February 1995 event are shown in Table 5.1.

Table 5.1

Soil Shear Moduli (ksf) Used for February 23, 1995 Event

Response Direction	Modulus Beneath Mat	Modulus to Side
X	4842	887
Y	5171	901
V	5500	1402

The comparisons between the computed and measured spectra for this earthquake are shown

on Figures 5.1 through 5.3 for the X, Y, and V directions respectively. The spectra of the measured motions are shown in bold lines while the spectra from the computed motions are shown with thinner lines.

The predicted X direction spectra do not compare well with the measured spectra (Figure 5.1) while the comparison between the Y direction spectra (Figure 5.2) is quite good. The predicted spectra are unconservative at the roof for frequencies greater than 3.5 cps as compared to the measured spectra while the predicted spectra. The predicted spectra in the Y direction are unconservative to a much lesser degree with the unconservative ranges restricted to narrow frequency bands. It is likely that the Standard Review Plan requirements for spectra broadening and consideration of a range in soil properties will eliminate the unconservative zones in the Y direction but not in the X direction. It is also interesting to note that the ZPA predicted values are lower than the measured values at the roof but higher at the basemat.

Peaks at three frequencies can be identified in the measured horizontal (X and Y) spectra. One occurs at about 5 cps and is the rocking SSI mode. This SSI frequency is reduced from 6 cps found from the forced vibration tests. This change implies that the soil shear modulus during the earthquake is about 70 % of the low strain values. This reduction is not consistent with soil shearing strains and degradation models. One possible explanation is that the backfill material is more effective for the forced vibration tests than it is for the seismic response problems. The backfill material is significantly stiffer than the virgin material. There is an amplification of the measured basemat motion at the roof elevation at this SSI frequency equal to about 5 in the X direction and about 4 in the Y direction. The amplification is about 2 in both direction for the predicted spectra. The other two peaks occur at frequencies of 1.5 cps and 3 cps. These peaks appear to be associated with the input motion. It is interesting to observe that both peaks occur in each of the spectra (X and Y).

The correlation of the computed and measured vertical spectra for the February event are shown on Figure 5.3. It may be seen that the correlations are fairly good except at frequencies of about 5 cps and 25 cps. The peaks of the measured spectra exceed the predicted spectra at 5 cps and the reverse is true at 25 cps. The forced vibration tests indicate that the vertical SSI frequency is about 15 cps and highly damped. It is not clear why the measured data shows a significant amplification (about 2) of the free field motion at 5 cps.

The soil properties used for the February 1995 event are shown in Table 5.1. These are somewhat lower than those found for the February 1995 earthquake because of the higher shear strains and corresponding higher degradation found for the May event.

Table 5.2

Soil Shear Moduli (ksf) Used for May 1, 1995 Event

Response Direction	Modulus Beneath Mat	Modulus to Side
X	4193	828
Y	4169	779
V	5500	1402

Comparisons of the computed and measured spectra in the X, Y, and V directions are shown on Figures 5.4, 5.5, and 5.6 respectively. These comparisons contain the same characteristics as discussed above for the February event. The SSI frequency appears to be reduced from 5 cps for the February earthquake to 4 cps for the May event. The amplifications (roof/basemat) of the measured data are reduced to 2.5 in the both the X and Y directions. Recall that these amplifications were 5 and 4 in the X and Y directions for the February earthquake. The amplifications of the predicted spectra are about 2 in both directions. The large amplifications of the vertical motions found at 5 cps for the measured data are significantly reduced resulting in a better correlation between the predicted and measured results for the May earthquake.

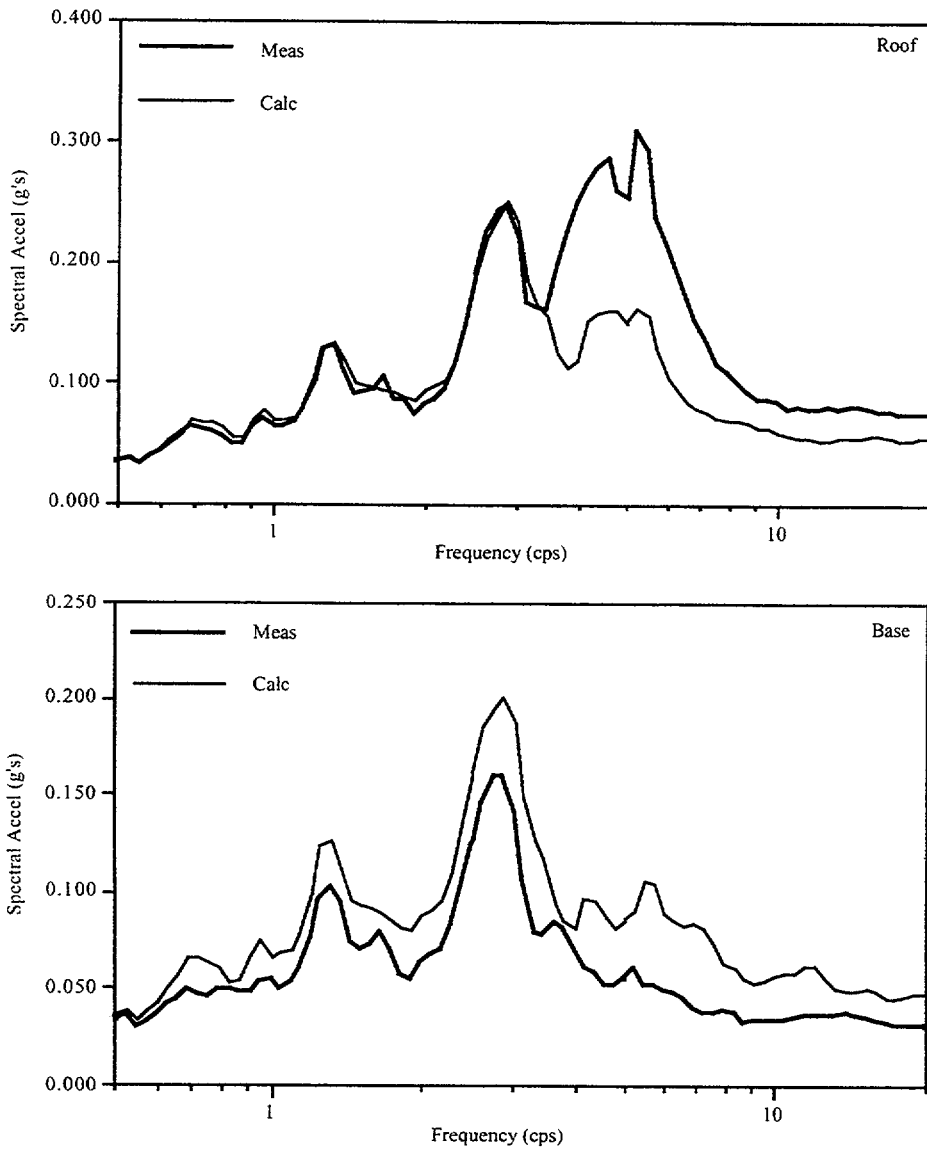


Fig. 5.1 Comparison of Computed with Measured Model X Spectra (5%); 2-23-95

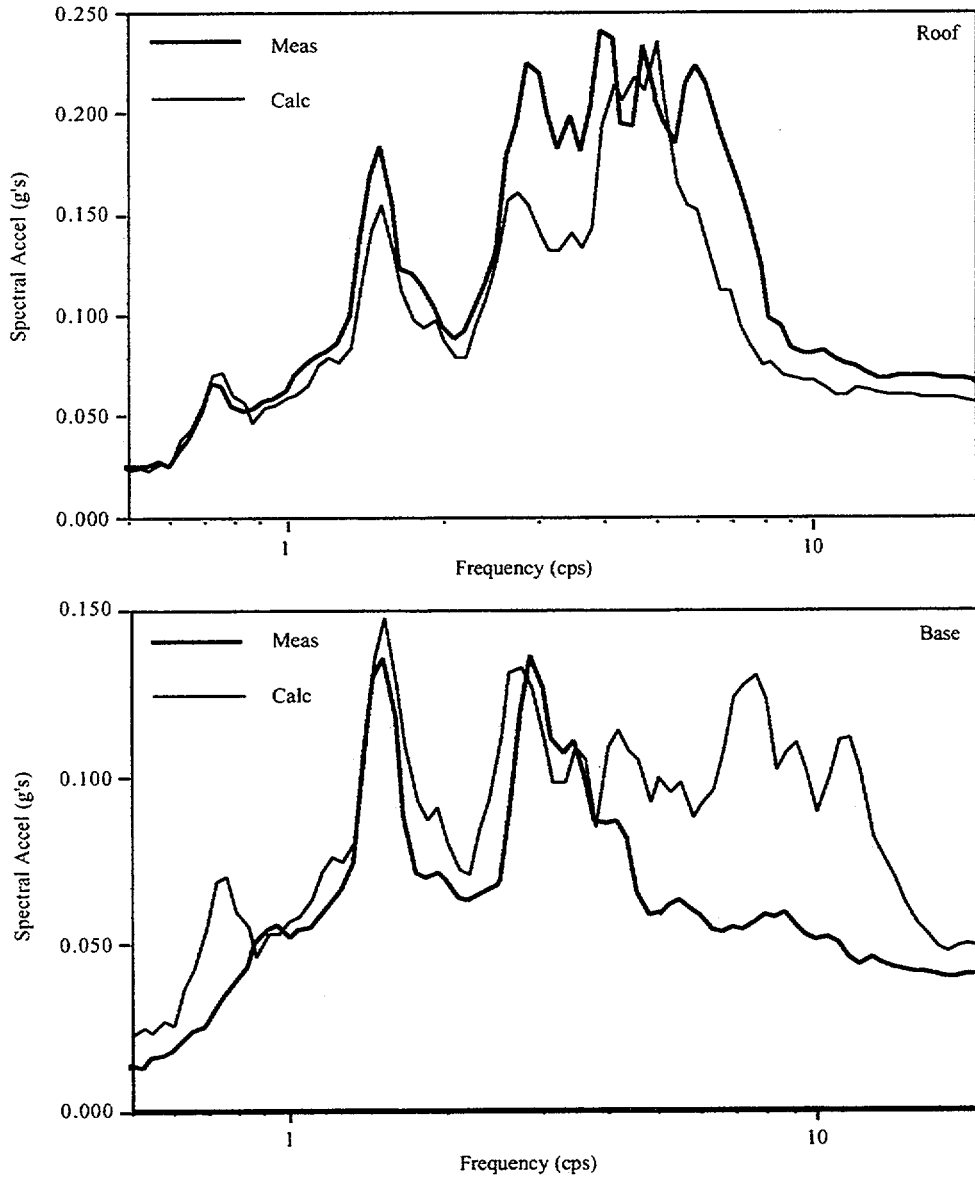


Fig. 5.2 Comparison of Computed with Measured Model Y Spectra (5%); 2-23-95

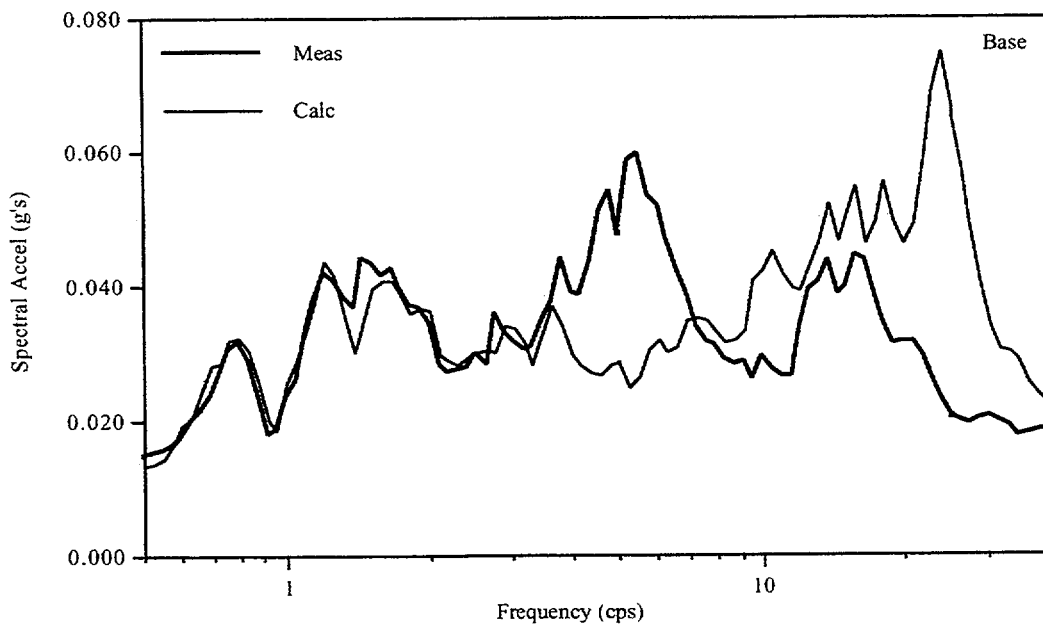
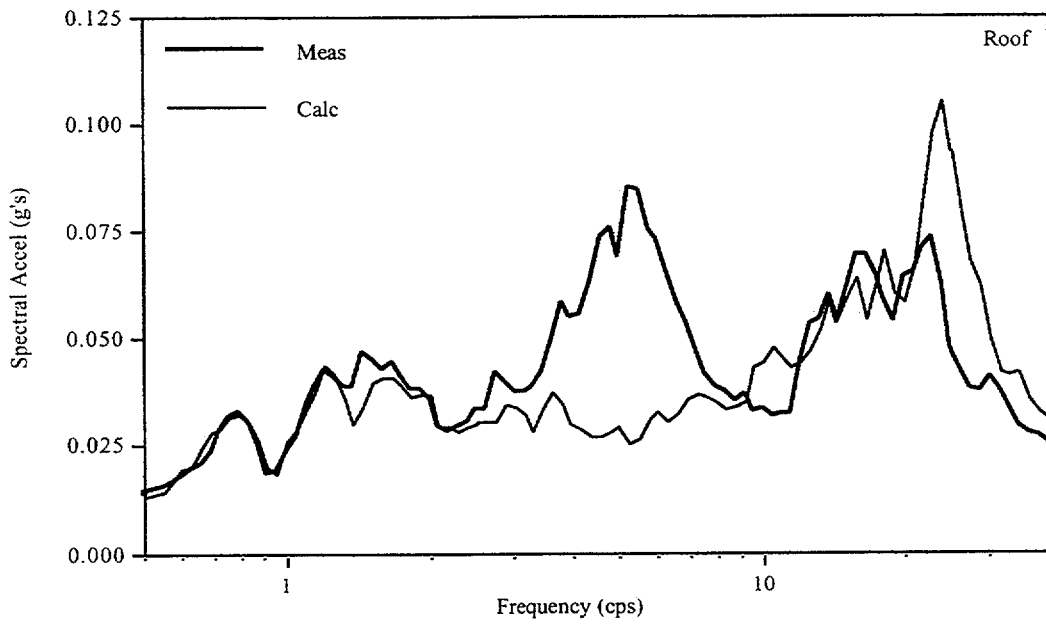


Fig. 5.3 Comparison of Computed with Measured Model V Spectra (5%); 2-23-95

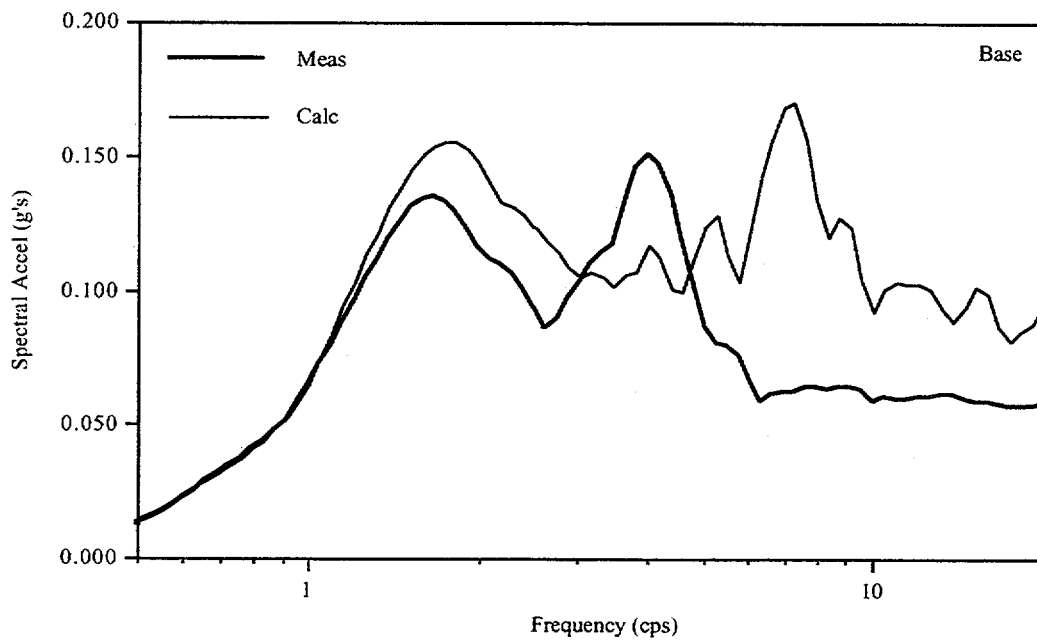
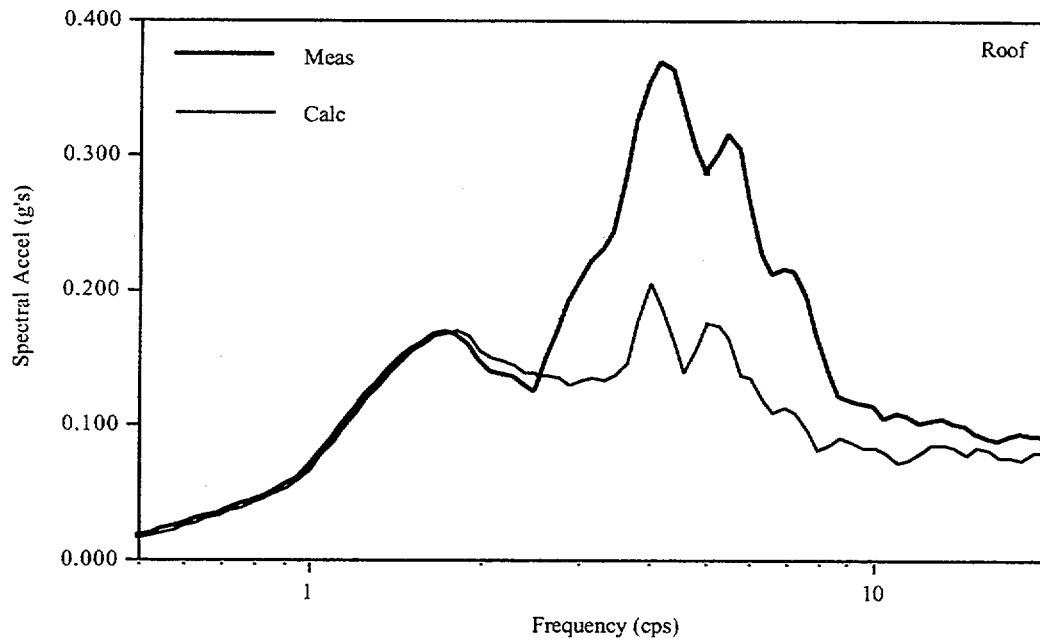


Fig. 5.4 Comparison of Computed with Measured Model X Spectra (5%); 5-1-95

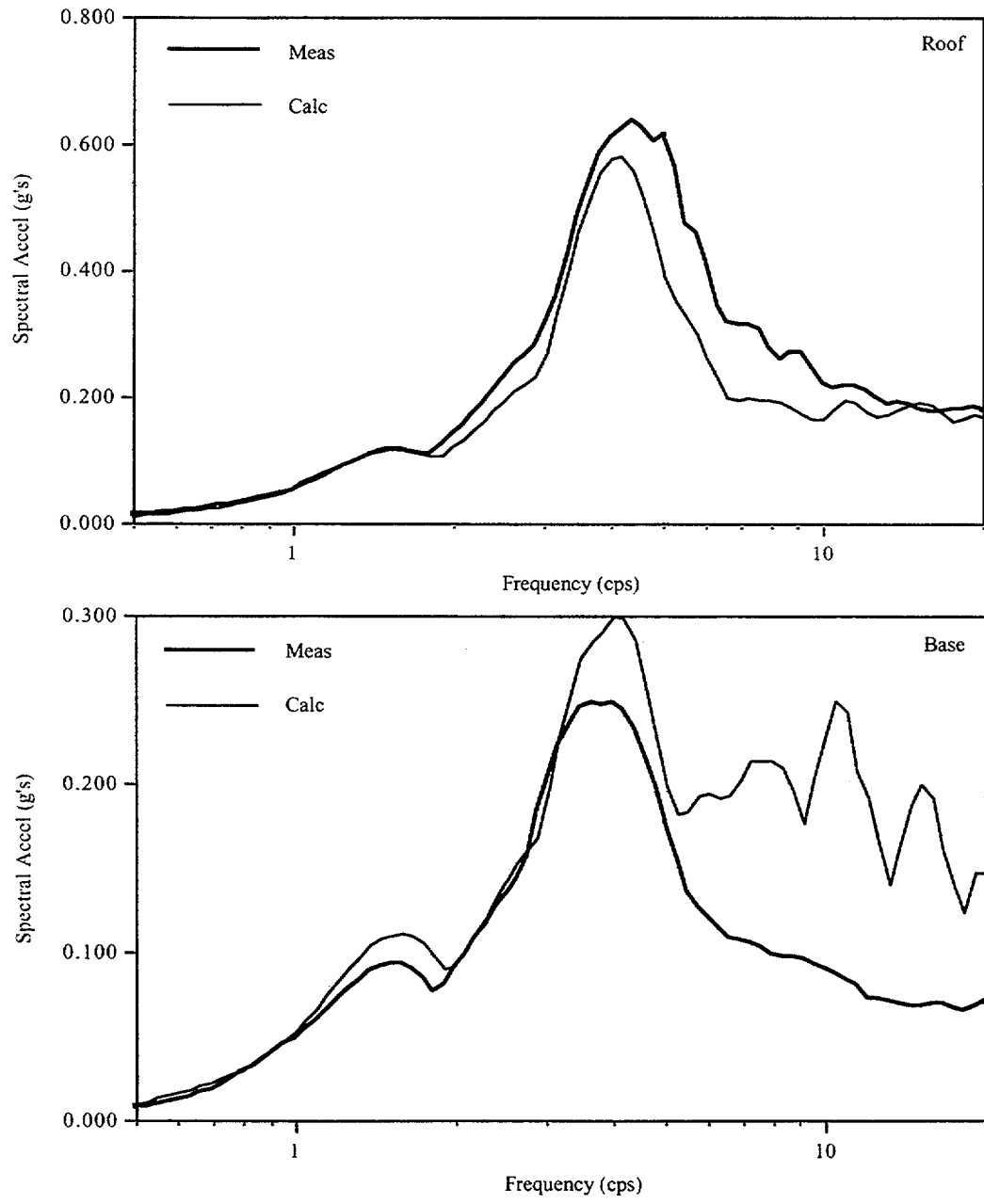


Fig. 5.5 Comparison of Computed with Measured Model Y Spectra (5%); 5-1-95

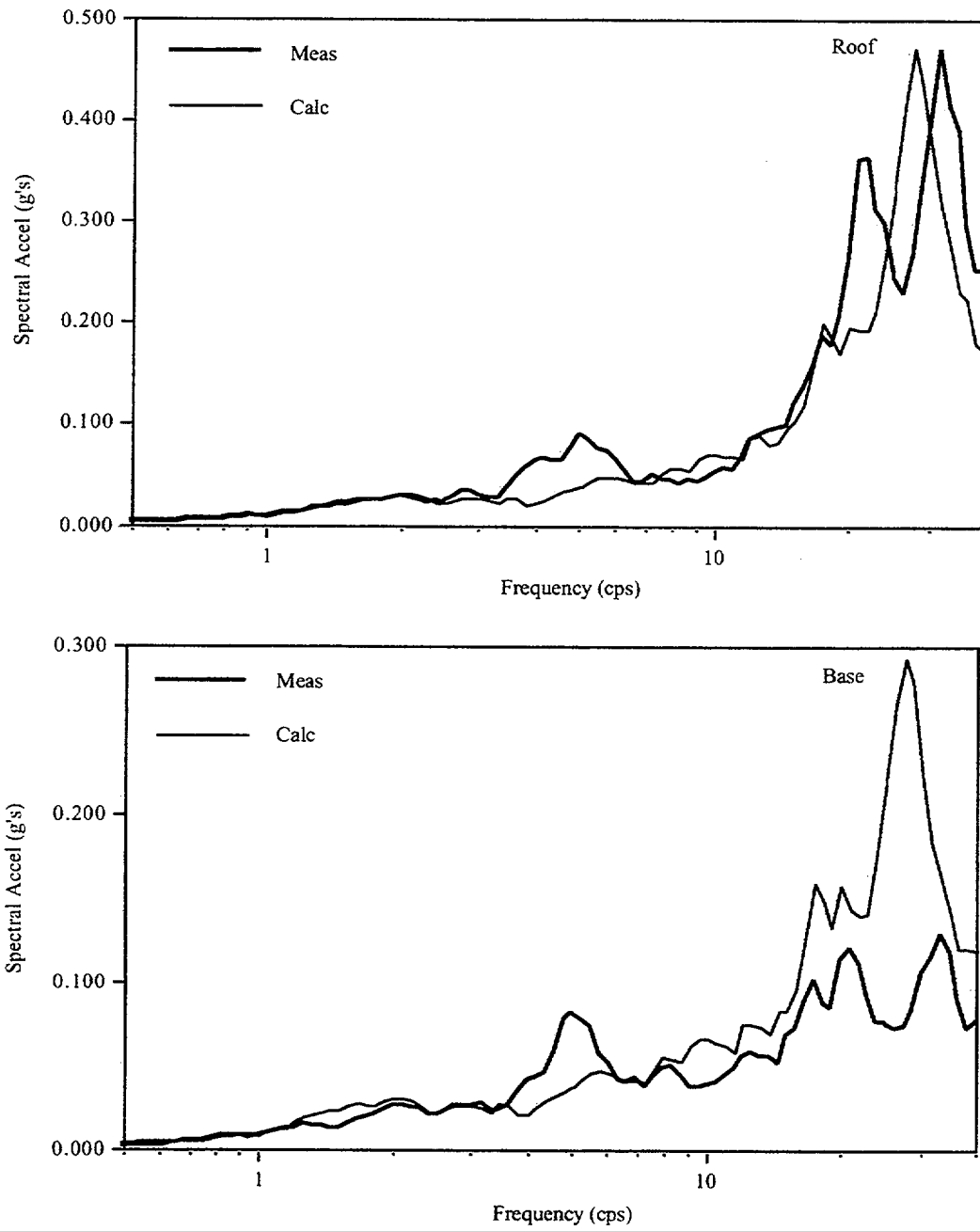


Fig. 5.6 Comparison of Computed with Measured Model V Spectra (5%); 5-1-95

6.0 Summary and Conclusions

This is the fourth of four volumes of the final report for the contract dealing with the review of the Hualien Large Scale Soil Structure Interaction experiment conducted in Hualien, Taiwan. Comparisons of the measured response in the free field and the model with predicted responses for a series of earthquakes are discussed in this volume of the report

Data recorded during four earthquakes are considered. Two of the earthquakes are magnitude 5.5 events and occurred about 22 km NE of the site. The peak recorded free field and in-structure accelerations during these events are 0.06 g's and 0.08 g's respectively. The other two events are magnitude 4.7 and occurred about 5 km from the site. One was located NE the site and the other SE of the site. The peak accelerations recorded are 0.14 g's and 0.17 g's in the free field and structure respectively. One earthquake from each is selected for detailed study (the magnitude 5.8 February 23, 1995 event and the magnitude 4.9 May 1, 1995 event).

A series of studies are performed using the measured data to obtain some insight to the significant characteristics of the model. In particular these studies were performed with the objective of evaluating the extent to which the earthquake data is consistent with the results of the forced vibration tests conducted after backfill. The forced vibration tests indicated that significant nonsymmetric responses occur (attributed to anisotropic site properties) and that the primary SSI frequency was 6 cps and associated with the rocking mode. The following is a summary of the studies and results:

1. Transfer functions are developed between the responses at the roof of the model and the surface gages in the free field. These transfer functions indicate that there is a significant coupling between the free filed horizontal input motion in the L and T directions and the model response. The measured data are used to determine principal directions which are found to be 29° east of the L direction. These principal directions are separated by about 10° from the principal directions as found from the forced vibration tests and confirm the anisotropic characteristics of the site.
2. Transfer functions between each of the gages in the downhole array are developed. This is done both in the L / T measurement coordinate system and in the principal X / Y system. The Transfer functions are found to depend on the direction giving further evidence of anisotropic effects. The frequency at which the initial peaks in the the transfer functions occur are in the order: Y>L>T>X. This indicates that the site is stiffer in the Y direction than in the X direction as was also found from the forced vibration tests. The fact that the stiffness in the L / T directions falls within the stiffness in the X / Y directions is also consistent with the determination that the X / Y coordinates represent principal directions.

It is also found that this anisotropic effect extends down to the deepest gages (between gage d27 at 86 feet and d28 at 170 feet). This supports the conclusion that the anisotropic characteristics are site wide and not restricted to a region around the model.

3. The fundamental frequencies in the soil column as found from the transfer functions support the conclusion that the soil may be softer than suggested in the CRIEPI unified soil model. In particular it appears that a soft layer in the soil column occurs somewhere between a depth of 52' (gage d 26) and a depth of 52 feet (gage d27).
4. Transfer functions between the roof of the model and the furthest surface free field gages (a15, a25, and a35) are found to depend on direction (X / Y or L / T) and on the free field gage used to define the control motion. The dependence on direction again reflects anisotropic site characteristics, and the dependence on location of the control point indicates that difficulty is likely to be encountered when attempting to predict the model response.

The CARES computer code is used to deconvolve the measured motion at gage a25 down to the four gages below (d25, d26, d27, and d28). This is done in the three directions X, Y, and V. The unified soil model properties are used with the soil moduli degraded and damping increased depending on soil strain and the degradation model included with the unified soil model. Spectra of the computed motion at the four gage locations are then compared with spectra of the recorded motion. The following conclusions are drawn from these comparisons:

1. Reasonably good agreements in the horizontal components of the motion are found over the entire depth of the soil column with the Y direction correlations being somewhat better than those in the X direction.
2. The correlations between the measured and computed spectra of the horizontal motions are better at gages d25 and d28 than at gages d26 and d27. This may result from the fact that the column frequencies above gages d26 and d27 are close to principal frequencies of the input motion (1.5 - 3 cps).
3. The correlations between the measured and computed vertical spectra are good at all depths for frequencies less than 10 cps. The computed spectral accelerations are higher than for the measured data at these higher frequencies.

The CARES computer code is also used to compute the model response given the measured free field motion at gage a25. The Beredugo - Novak soil structure interaction model is used. This is done in the three directions X, Y, and V. The unified soil model properties are used with the soil

moduli degraded and damping increased depending on soil strain and the degradation model included with the unified soil model. Spectra of the computed motion at the roof and base are then compared with spectra of the recorded motion. The following conclusions are drawn from these comparisons:

1. The correlations between the spectra developed from the predicted and measured response are poor for the X direction motion and good for the Y direction motion.
2. The predicted roof spectra in the X direction are unconservative for frequencies greater than 3.5 cps. The predicted spectra in the Y direction are unconservative in rather narrow frequency bands. It is unlikely that the Standard Review Plan requirements for broadening the spectra and using a range in soil properties would eliminate the region in which the X spectra are unconservative, but likely would eliminate these regions for the Y direction spectra.
3. The forced vibration tests after backfill indicated that the fundamental vibrational mode of the soil / structure system is a rocking mode at a frequency of 6 cps. The fundamental mode for the February and May earthquakes are 5 cps and 4 cps respectively. This reduction in frequency is larger than would be anticipated based on degradation effects on the soil shear modulus.
4. The correlation between the computed vertical motion spectra and the spectra for the measured motion are good at all frequencies except around 5 cps and 25 cps. The predicted values are conservative at 25 cps and unconservative at 5 cps.

References

1. H. T. Tang, "Large Scale Soil Structure Interaction Report," Electric Power Research Institute, Report NP-5513-SR, 1987.
2. J.Xu, A.J. Philippacopoulos, C.A. Miller, and C.J. Costantino, "CARES (Computer Analysis for Rapid Evaluation of Structures) Version 1.0," NUREG/CR-52241, Brookhaven National Laboratory, July 1990.
3. Y.O. Beredugo, and M. Novak, "Coupled Horizontal and Rocking Vibration of Embedded Footings," Canadian Geotechnical Journal, 1972.

BIBLIOGRAPHIC DATA SHEET

(See instructions on the reverse)

1. REPORT NUMBER
(Assigned by NRC, Add Vol., Supp., Rev.,
and Addendum Numbers, if any.)

NUREG/CR-6584

2. TITLE AND SUBTITLE

Evaluation of the Hualien Quarter Scale Model Seismic Experiment
Volume 4

3. DATE REPORT PUBLISHED

MONTH	YEAR
March	2001

4. FIN OR GRANT NUMBER

W6769

5. AUTHOR(S)

C. A. Miller, C. J. Costantino

6. TYPE OF REPORT

Final

7. PERIOD COVERED (Inclusive Dates)

3/92 to 10/99

8. PERFORMING ORGANIZATION - NAME AND ADDRESS (If NRC, provide Division, Office or Region, U.S. Nuclear Regulatory Commission, and mailing address; if contractor, provide name and mailing address.)

The City College of New York
Department of Civil Engineering
New York, NY 10031

9. SPONSORING ORGANIZATION - NAME AND ADDRESS (If NRC, type "Same as above"; if contractor, provide NRC Division, Office or Region, U.S. Nuclear Regulatory Commission, and mailing address.)

Division of Engineering Technology
Office of Nuclear Regulatory Research
U. S. Nuclear Regulatory Commission
Washington, DC 20555-0001

10. SUPPLEMENTARY NOTES

Herman L. Graves, Project Manager

11. ABSTRACT (200 words or less)

A quarter scale model of a containment structure was constructed in Hualien, a seismically active region in Taiwan. Forced vibration tests were performed both before and after placement of the backfill. The structure and surrounding free field were then instrumented with accelerometers, pressure gages, and displacement gages. Recordings were taken when significant seismic events occurred at the site. This report describes analytical studies that were performed to correlate the measured response with predictions. Soil - structure interaction effects were represented with a lumped parameter model.

The work is summarized in Volume 1 of the 4 volume report. The site characteristics are described in Volume 2. This includes a discussion of the field program used to determine the characteristics. The predictions for the forced vibration tests are compared with the measured data in Volume 3. The correlation is found to be quite good except that the measured data indicated that the site is anisotropic. This is not found from the site exploration phase of the work. Comparisons between the predictions and measured data for the earthquake responses are made in Volume 4. The soil responses compare reasonably well but the in structure responses do not compare very well. This is attributed to the anisotropic site characteristics.

12. KEY WORDS/DESCRIPTORS (List words or phrases that will assist researchers in locating the report.)

Hualien, soil-structure interaction, shear wave velocity, forced vibration

13. AVAILABILITY STATEMENT

unlimited

14. SECURITY CLASSIFICATION

(This Page)

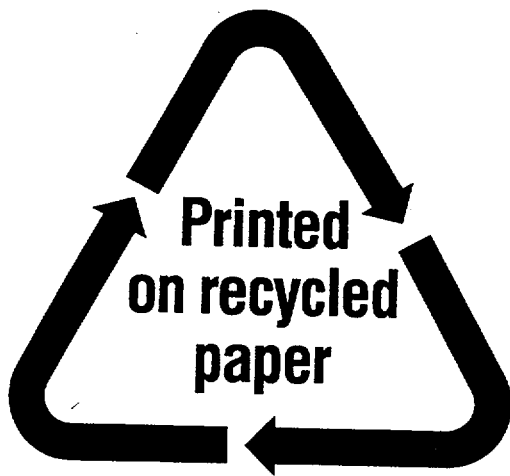
unclassified

(This Report)

unclassified

15. NUMBER OF PAGES

16. PRICE



Federal Recycling Program

UNITED STATES
NUCLEAR REGULATORY COMMISSION
WASHINGTON, DC 20555-0001

OFFICIAL BUSINESS
PENALTY FOR PRIVATE USE, \$300